

Article

A New Mode of a Natural Convection Solar Greenhouse Dryer for Domestic Usage: Performance Assessment for Grape Drying

M. A. Tawfik, Khaled M. Oweda *, M. K. Abd El-Wahab and W. E. Abd Allah

Agricultural Engineering Department, Faculty of Agriculture, Zagazig University, Zagazig 44511, Egypt; mayosif@zu.edu.eg (M.A.T.); mkhasanien@agri.zu.edu.eg (M.K.A.E.-W.); wesam@zu.edu.eg (W.E.A.A.)

* Correspondence: km.elsayed23@agri.zu.edu.eg

Abstract: It is known that the natural convection (NC) solar drying process is a simple and cheap method for drying foodstuffs, but it is not preferable for common users in the case of drying high-moisture content agro-products due to the slow rate of drying. Meanwhile, the forced convection (FC) drying process is most appropriate for such products, but its economic feasibility may be affected due to high initial and maintenance costs. Therefore, the present study proposed a controlled natural convection (CNC) drying mode using a solar greenhouse dryer (SGD) for drying grapes with two types of cover materials, glass and Plexiglas, through intermittent operation with a PV system to save energy as a simple and inexpensive domestic dryer instead of the common forced convection SGD and the conventional natural convection SGD. The obtained results of the new CNC drying mode using a Plexiglas SGD showed a higher drying rate than the NC drying mode and are close to the FC drying mode using the same cover material. The initial moisture content of the grapes was reduced from 5.91 g water/g dry matter to the final moisture content of 0.15 g water/g dry matter within 12 h and 15 h for the CNC and NC drying modes, respectively, using the Plexiglas SGD. Moreover, the thermal drying efficiency for the two mentioned drying modes was 12.5 and 9.7%, respectively. The Page model was found to be the most appropriate model to predict the kinetics of the SGD in all drying modes, regardless of the cover type. The new CNC drying mode using the Plexiglas SGD achieved the lowest cost per kg of dried grapes (1.26 USD/kg), the highest total saved costs over the lifespan of the dryer (USD 245.46) and the shortest payback period (1.08 years) compared to the other two dryers, NC-SGD and FC-SGD. Generally, the CNC-SGD had good performance over the NC-SGD because it is not affected by the fluctuation in the volume, velocity and direction of the inlet ambient air/wind during drying grapes as a high-moisture content product without external heating sources or complicated parts. Thus, the proposed drying system has the advantage in terms of simplicity, cheapness and saving energy compared to FC-SGD.



Citation: Tawfik, M.A.; Oweda, K.M.; Abd El-Wahab, M.K.; Abd Allah, W.E. A New Mode of a Natural Convection Solar Greenhouse Dryer for Domestic Usage: Performance Assessment for Grape Drying. *Agriculture* **2023**, *13*, 1046. <https://doi.org/10.3390/agriculture13051046>

Academic Editors: Kristina Kljak, Klaudija Carović-Stanko, Darija Lemić, Jernej Jakše, Kurt A. Rosentrater, Arup Kumar Goswami and Craig Sturrock

Received: 16 April 2023

Revised: 8 May 2023

Accepted: 10 May 2023

Published: 12 May 2023



Copyright: © 2023 by the authors. Licensee MDPI, Basel, Switzerland. This article is an open access article distributed under the terms and conditions of the Creative Commons Attribution (CC BY) license (<https://creativecommons.org/licenses/by/4.0/>).

Keywords: solar greenhouse dryer; grape drying; new drying mode; controlled natural convection; thermal performance; drying kinetics

1. Introduction

Simply put, the availability of energy is considered key to the progress and flourishing of any nation on the level of health, education, industry and economy [1]. At the same time, the global population was 8 billion in 2022, and is predicted to reach 9.7 billion in 2050 [2]. Thus, societies around the globe will necessarily be subject to major challenges regarding energy and water demands alongside the food supply and security. Utilizing and implementing renewable energy sources is the most effective, green and sustainable path to mitigate greenhouse gases (GHG), which contribute to global warming [3].

The drying process is one of the most simple and widely used processes as a preservation technique for agro-products. It helps to increase shelf life, improves quality and reduce losses during storage [4,5], in addition to providing advantages to the dried products such as making them lightweight and easy to store, transport and use [6]. Generally, the drying

techniques available globally can be classified based on the source of heat into open-sun or natural drying, firewood (biomass) drying, fossil fuel drying, electrical drying and solar drying [7,8]. Farmers have used open-sun drying since ancient times as an energy-free and cheap method for drying their agro-products. However, this method has several disadvantages, such as (i) needing a large occupation space and long drying time [9], (ii) suffering from a loss of quality [10], (iii) heavy thermal energy losses [11], (iv) uncontrolled drying process [12] and (v) poor final products due to contamination by dust and dirt as well as the attacks of insects, birds, rodents and domestic animals [13–16]. The drying process in the industrial sector is an intensive energy-consuming operation because it requires a massive amount of thermal energy for heating and dehydrating products [17]. Generally, the thermal drying process consumes about 10–20% of the industrial sector’s total energy consumption in developed countries [18]. Nevertheless, a significant part of the world’s total energy consumption (about 30%) comes from the agricultural sector, of which ~4% is used for drying agricultural products [19]. Hence, the drying sector is a big consumer of energy [20]. In light of this, the use of large amounts of fossil fuels in the drying process to meet the required heat for this sector leads to major concerns from economical and environmental perspectives. The high preliminary and running costs of fossil fuel-driven dryers are considered a big barrier for small-scale farmers to accept such dryers [21]. The farmers usually cannot afford fossil fuel-powered dryers due to their high capital and operating costs in developing-economy countries [22]. In these countries, 80% of food is produced by small farmers [23].

Solar dryers can be classified based on the hot air circulation method/or operation mode, the mode of heat transfer to the product and the dryer’s design (Figure 1).

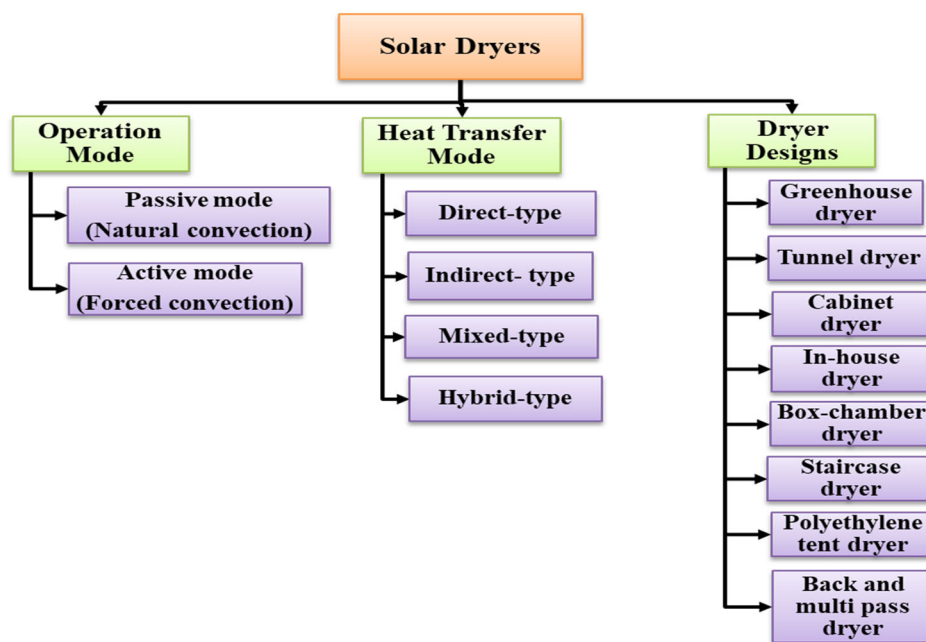


Figure 1. Solar dryer classification from [24,25].

Out of the various solar drying methods, the solar greenhouse dryer (SGD) is one of the oldest and most widespread methods for crop preservation [26] as a sustainable option for drying products due to its low cost and energy savings [27]. SGDs work on the concept of the greenhouse effect by trapping long-wave solar radiation within the dryer to produce the heat required for drying [28]. SGDs offer a controlled environment for the drying process in terms of the relative humidity and temperature required for shortening the drying time, making them more suitable for crop drying [29].

Moreover, SGDs are widely accepted by farmers due to their large capacity and low operational costs. The low or no power requirement makes such a type of solar dryer

a prospective option for installation on farms in remote areas [30]. Therefore, SGDs are classified as direct-type dryers based on the heat transfer mode through which the moisture content can be removed, either by the natural or forced convection mode. If they are combined with a solar air heater and solar panels, they come under the mixed-mode and hybrid types [31]. They can be used throughout the year, making them more effective regarding the economic aspect. The payback period of an SDG is about ~2.5 years [32]. The natural-mode greenhouse drying process depends on the thermosyphon effect theory. At the same time, an exhaust supports the SGD, which operates under the forced convection drying mode with fan installation to ventilate the humid air from the drying chamber [33]. The forced convection mode for SGDs offers better control and optimum drying conditions inside the dryer with the help of a fan or blower [34]. The natural convection mode for SDGs is used for relatively low-moisture content crops, whilst forced-mode SGD is used for high moisture content crops [35]. One of these crops is grapes due to their high moisture content.

Grapes have various advantages such as high nutrient levels and antioxidant content that may protect against chronic diseases such as diabetes and certain types of cancer, as well as reducing the blood sugar [36]. Grapes are perishable fruit with a high moisture content. The proper and efficient drying method plays a vital role in storing such perishable fruits for a long period in the form of raisins with high-quality properties that are needed for better market value. In the last two decades, limited studies have investigated drying grapes using different operation heat transfer modes. These works include using an indirect cabinet solar dryer under forced convection with a solar air heater (SAH) [37–41], a set of SAHs [42], combined SAH with an electrical heater [43,44], mixed-mode [38,45,46] and a mixed-mode natural convection dryer with PCM [47,48]. Despite the efficacy of indirect solar dryers for drying grapes, SGDs are still more efficient for dehydrating grapes in a considerably short time due to the natural greenhouse effect inside SGDs. In the literature, few studies focused on drying grapes using SGDs (Table 1).

Table 1. Previous studies focused on grape drying using SGDs.

Reference	Location	Shape of SGD/ Cover Type	Operating Mode	Max. Solar Radiation/Avg- Temperature inside SGD	Variety of Grape (Pre-Treatment Solution)	Load/Drying Range and Time	Drying Efficiency
El Khadraoui et al. [31]	Borj Cedria, (36°43' N, 10°25' E), Tunisia	Chapel-shaped/Plexiglas	Mixed-mode forced convection using flat plate SAH	~808 W/m ² /49.88 °C	Sultana (1% NaOH)	130 kg/From 5.49 gWater/g dry matter to 0.22 (gWater/g dry matter) in 30 h	N.A
Fuller and Charters [49]	Northern Victoria (35° 57' S 144° 36' E) Australia	Tunnel-shaped/Polyethylene sheets, two layers	Forced convection	~23 MJ/m ² /60 °C	Sultana (untreated)	From 76% to 13% in 288 h	15–17%
Barnwal and Tiwari [50]	New Delhi (28° 35' N, 77° 12' E), India	Roof type even span/ Polyethylene sheets	Hybrid PV/T Forced convection	N.A	Thompson Seedless (untreated)	8 kg/(N.A)	38.40–43.6%
Rathore and Panwar [51]	Udaipur (27° 42' N, 75° 33' E), India	Tunnel-shaped/Polyethylene sheets	Natural convection	~950 W/m ² /-65 °C	Thompson Seedless (untreated)	320 kg/From 85% to 16% in 168 h	30%
Hamdi et al. [52]	Borj Cedria, (36°43' N, 10°25' E), Tunisia	Chapel-shaped/Plexiglas	Mixed flow/Forced convection	795 W/m ² /28.08 °C–55.94 °C	Sultana (treated with 1% NaOH)	130 k/From 5.5 g water/g dry matter to 0.22 (g water/g dry matter) in 128 h	N.A
Tiwari et al. [53]	New Delhi (28° 35' N, 77° 12' E), India	Single-slope PV/T solar greenhouse dryer	Hybrid PV/T Forced convection	~890 W/m ² /-60 °C	Seedless (N.A)	N.A/1618 gWater to 594 gWater in 144 h	15–30%
Gopinath et al. [54]	Tamil Nadu (9°34' N, 77°40' E), India	Parabola-shaped/Poly-carbonate	Forced convection	N.A/45 °C for without PCM, 47.50 °C for with 100 g PCM and 58 °C for 200 g PCM	Seedless (treated with 6% K ₂ CO ₃ and 0.5% olive oil)	N.A/From weight 80.20% –18.60% -Without PCM = 34 h -With PCM 100 g = 22 h With PCM 200 g = 10 h	N.A
Nagarajan and Premkumar [55]	Coimbatore-Tamil Nadu (11° N, 76° 57' E), India	Tunnel-shaped/poly-carbonate	Forced convection using SAH	~830 W/m ² /35 °C–75 °C	Grapes (variety not determined)	1 kg/From 75% to 7% within 48 to 72 h	N.A

The perishable and high moisture content of agro-products such as grapes is prolonged due to the waxy layer that covers the grape peel [56]. Thus, the forced-convection SGD (FC-SGD) is mostly suitable for grapes. In this mode, the SGD is often augmented with heating auxiliaries such as air solar collectors/heaters, electrical heaters or mixed modes for operation, as well as using PCM for drying grapes to produce raisins. However, these methods may harm the drying process from the economic aspect, which can reduce the propagation of SGDs worldwide.

The available literature in Table 1 shows that the natural convection SGD (NC-SGD) or the passive mode is rarely used as a sole operation mode without augmentation of auxiliary heating systems for drying the mentioned products. Thus, the challenge of using NC-SGD for drying such high-moisture content agro-products in an efficient way and short time will be raised against the end users, who prefer utilizing NC-SGD due to its advantages including high capacity, low installation cost and operational costs that suit small-scale farms. Therefore, there is an urgent need for more exploratory works to develop, enhance and assess the performance of such inexpensive NC-SGD to be exploited for drying perishable high-moisture agro-products for small-scale domestic drying purposes powered by solar energy to suit the population disconnected from the grid in rural, remote and isolated areas.

In light of the above, the novelty of this work is presenting a new drying mode of natural convection SGD for drying high-moisture content agro-products (i.e., grapes) as a standalone drying system for domestic purposes in an attempt to avoid the drawbacks NC-SGD represents in terms of a slow drying process as well as the high installation operation and maintenance of FC-SGD. The proposed system was provided with an automatic control unit (ACU) to keep the parameters of the internal environment inside the dryer at an appropriate level during typical days for drying grapes without using an external heating source (i.e., solar collectors, heaters, etc.) or complicated parts. Therefore, the new proposed drying system will not be affected by fluctuations in the volume, velocity and direction of the ambient air/wind even in the late hours of the drying period. Moreover, the new drying mode of using controlled natural convection SGD (CNC-SGD) will allow the user to avoid tracking the direction of ambient air/wind that may occur when using CN-SGD. Additionally, the proposed drying system has the advantages of simplicity, cheapness and saving energy due to intermittent operation compared to the FC-SGD,

Hence, the objectives of the present work are to (i) fabricate an even-span-type solar greenhouse dryer (SGD) from two different materials, glass and Plexiglas, as well as evaluate its thermal performance for drying grapes under different operational modes; (ii) establish a simple, low-cost and easy-to-operate passive dryer as a new operational mode for solar drying that will be called hereafter the controlled natural convection SGD (CNC-SGD), which represents the novelty of the present work; (iii) compare the thermal performance of the new mode CNC-SGD to the forced convection (FC-SGD) and conventional natural convection (CN-SGD) drying modes in terms of thermal performance, drying kinetics and drying efficiency and (iv) perform an economic assessment to determine the best drying mode from an economic perspective.

2. Materials and Methods

2.1. Solar Drying Setup

In the present study, three operational modes of SDG were used to produce raisins through solar drying of seedless grapes of the Sultana variety on a small scale and for domestic purposes. Two different materials for fabricating SDG were tested; glass and Plexiglas (transparent acrylic glass). The three operational modes were used, including the conventional natural convection drying mode, forced convection drying mode and the new fully controlled natural convection mode. The two SGDs were fabricated and developed at a private workshop at the location of experiments in Zagazig City, Egypt (30.57° N latitude, 31.50° E longitude) throughout the summer season of 2021. The SGD had a loading capacity of about 1.500 kg of grapes. This study's main components of solar drying systems included the SGD, a solar air heater, PV system and automatic controller with sensing system.

2.1.1. Solar Greenhouse Dryer (SGD)

The practical experiments were conducted in two identical even-span-type SGDs that were fabricated and tested simultaneously to evaluate their effects on drying efficacy in the different mentioned drying modes. Each dryer had a 1.20 m length, 0.60 m width,

0.60 m height for the vertical wall and 0.75 m height from the center. Each SGD had a drying chamber containing a wooden table covered with woven mesh made of stainless steel with dimensions of 110 cm L \times 45 cm W to hold the grapes at 40 cm above the floor of the chamber. The drying chamber's floor was made of two wooden sheets, each 3 cm in thickness, and packed with 5 cm of glass wool as an insulator to reduce heat losses from the drying chamber floor to the surroundings. A kind of porous cloth (fabric material) was placed on the woven mesh to circulate air from the bottom to the top of the drying chamber and then to the air vent located on the top roof of SGD. The rooftop and walls of the SGD were covered either by glass or Plexiglas sheets with the same thickness, 5 mm. The used SGDs were oriented in the east–west direction.

2.1.2. Solar Air Heater (in Case of Forced Convection Drying Mode)

The heater mainly consisted of a rectangular wooden container (120 cm length, 60 cm width, 20 cm Depth), a transparent glass cover of 5 mm in thickness sealed to the wooden container using thermal silicon, an absorber plate with welded metallic pipes (heating pipes) and a compact 10 cm layer of glass wool packed into the gap between the back internal side of the wooden container and the bottom surface of the absorber. As seen in Figure 2, the enclosure of the SAH was divided into two parts; the first one was the upper part, which represented the hot air collecting chamber that received the hot air from the heating pipes. This upper chamber was provided with a built-in centrifugal DC fan (power 10.56 W and diameter of 80 mm) to stream the desired flow rate of hot air into the SGD. This can be achieved by changing the fan speed through a controllable dimmer (speed regulator). The fan was installed at the bottom of the collecting air chamber on an outlet hole 8 cm in diameter connected to an insulated thermal duct with the same diameter to transfer the hot air from the hot air chamber to the drying chamber. The absorber occupied the second part, with welded metallic pipes that were placed 2 cm beneath the glass cover. A total of 40 pipes made of copper 100 cm in length and 2.54 cm in diameter were welded to the absorber plate (120 cm length, 60 cm width, 0.2 cm thickness), which was also made of copper. The pipes and absorber plate were painted with synthetic black matt paint. Each pipe was connected to a circular air intake hole with the same diameter allocated at the bottom side of the SAH; thus, there were 40 intake holes for the easy intake of ambient air into the heating pipes.

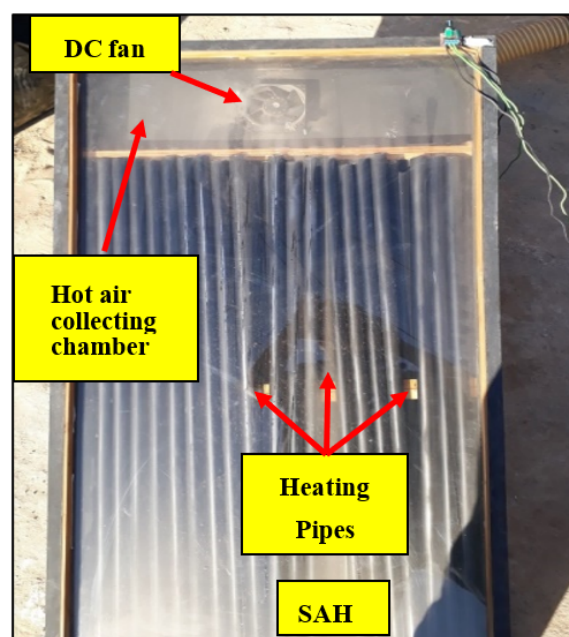


Figure 2. Photograph of SAH used for forced convection drying mode.

2.1.3. PV System

In the present study, a PV system was used to control two drying modes, the forced convection mode and the fully controlled natural convection mode. The PV system consisted of a polycrystalline photovoltaic (PV) solar module with a maximum power of 40 W (model SLP070-12U), a total surface area of 0.382 m² and a maximum efficiency of 19%. The solar PV module was rated by its DC output power. The PV module and its specifications are detailed in Table 2.

Table 2. The specifications of the solar PV module.

Parameters of PV Module	Specifications
Type	Polycrystalline Silicon
Dimensions (mm)	651 L × 526 W × 35 T
Weight (g)	5500
Maximum Power, P_{max} (W)	40
Optimum Operating Voltage, V_{MP} (V)	17.40
Optimum Operating Current, I_{mp} (A)	2.48
Open Circuit Voltage, V_{OC} (V)	21.70
Short Circuit Current, I_{sc} (A)	2.56

The output voltage of the PV module was set by a voltage regulator (with a maximum of 5 A). It stabilized the solar panel's outside voltage to reach 12 volts to protect the centrifugal fans from increased voltage difference and damage. A dimmer (speed regulator) was used to control the speed of forced blowing air (in the case of the forced convection drying mode).

2.1.4. Automatic Control Unit (ACU)

The new drying mode of fully controlled natural convection is considered an attempt to achieve the advantages of the conventional natural convection drying process, including the cheapness and simplicity in design and low initial and running costs. Meanwhile, the new drying mode aims to eliminate drawbacks of the conventional mode such as the full dependence on the ambient air velocity, the continuous orientation to face the wind direction and the long drying time for high-moisture content products (e.g., grapes). Moreover, the new drying mode aims to reduce the fabrication, repair and maintenance of the auxiliary parts required for the forced convection drying mode. Thus, an automatically controlled unit (ACU), Figure 3, was designed and retrofitted with the conventional natural convection SGD to control the operation of an air vacuum fan installed on the outlet vent.

The motherboard is considered the head of a system, as depicted in Figure 3. The ACU switched the fan on or off according to the pre-adjusted programmed temperature and humidity to ensure constant environment conditions inside the dryer to make the SGD independent of fluctuations in the ambient conditions.

According to the description of the ACU components (Table 3), the output voltage of the PV module was set by a voltage regulator to a maximum of 15 V. This suited the consumption of the ACU. Then, a voltage regulator (7805) was fixed in the unit to regulate the DC current to 12 volts for the DC vacuum fan consumption.

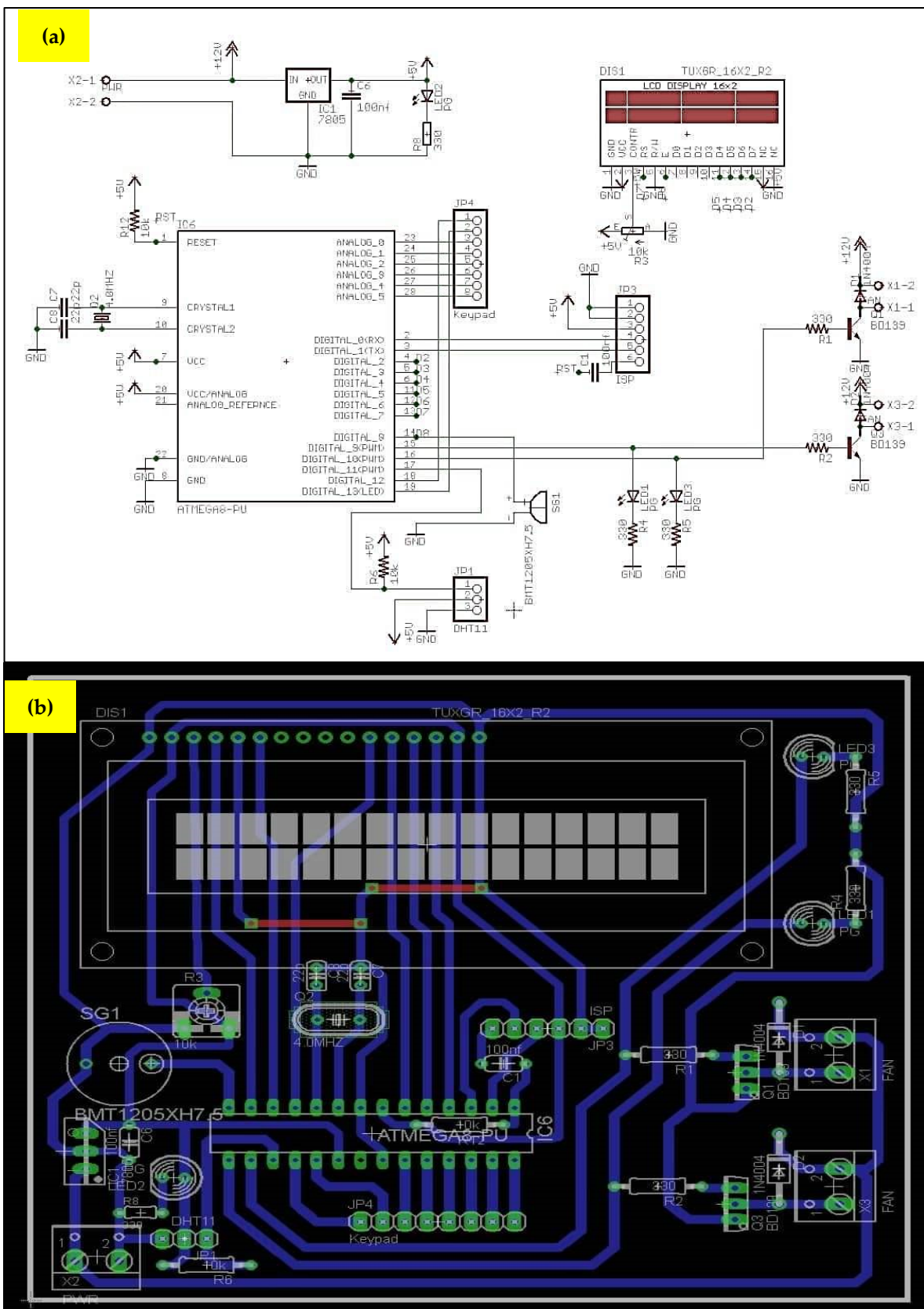


Figure 3. Views of: (a) electronic circuit, (b) the motherboard of ACU.

Table 3. The ACU components.

SI No.	Component	Description
1	LCD 16 × 2	Display of module
2	ATMEGA 328p	High-performance, low-power AVR® 8-bit microcontroller
3	Crystal oscillator 16 MHz	Designed to handle off-chip crystals that have a frequency of 4–16 MHz
4	Voltage regulator 7805	<ul style="list-style-type: none"> • 5 V positive voltage regulator • Minimum input voltage is 7 V • Maximum input voltage is 25 V • Operating current(I_Q) is 5 mA
5	Transistor BD 139	Designed for audio amplifiers and drivers utilizing complementary or quasi-complementary circuits
6	Capacitor 22p	Used with crystals for loading purposes
7	Red LED	Indicator
8	DHT 11	Temperature + humidity sensor
9	Keypad 4 × 4	<ul style="list-style-type: none"> • Maximum voltage across each segment or button: 24 V • Maximum current through each segment or button: 30 mA • Maximum operating temperature: 0 °C to + 50 °C • Ultra-thin design • Easy interface • Long life
10	Fan	Air ventilation fan (Exhaust fan)

The ACU was linked to a sensor installed inside the enclosure of the solar greenhouse dryer to detect the temperature and relative humidity of the interior air. The ACU was adjusted in advance to a particular temperature (55 °C) as the average maximum value from earlier works presented in Table 1, as was the relative humidity (max. 50%). The exhaust vacuum fan operated automatically to expel the internal drying air into the ambient area once the temperature or relative humidity of the interior air reached its pre-adjusted programmed value to avoid the accumulation of humid air inside the dryer or the over-drying phenomena due to the excess temperature of the internal air.

2.2. Experimental Procedure

In the present study, seedless grapes (Sultana variety) were dried to produce raisins. A sample of grapes was selected after separating their bunch and discarding the stems as well as the spoiled grapes. The selected grapes were washed with water to clean them of the dust and filth that may be stuck on grapes. After that, the grapes were pretreated by soaking them in an alkali solution of NaOH 5%, and then they were heated to a temperature of 90° for 30 s. This process was repeated consecutively three times to crack the grapes' peel. This process is essential to shorten the drying time by increasing the water permeability of the grapes' peel [57]. Afterwards, the grapes were washed with fresh water at ambient temperature and dried with a clean cotton cloth. Then, the pretreated grapes were distributed in a thin layer on the metallic mesh that was located within the SGD. The sample of dried grapes was weighed using a digital electronic balance (WANT balance) every 4 h throughout the drying period to determine the moisture loss. However, there were no measurements taken at night for the consecutive drying days, wherein the partially dried grapes were left inside the dryer throughout the night of the consecutive drying days with an insulation blanket. At the end of each experiment, the dried products were packed in polyethylene bags and stored at −4 °C prior to laboratory analysis [58]. The dry matter of grapes was determined by placing the dried product in an oven for 12 h at 120 °C [31]. All the experiments of the present work were carried out on clear and sunny days throughout the months of July to August 2021, from 8:00 am to 4:00 pm on the typical experimental days. When the drying process started, the fresh grapes had an average

moisture content on dry basis of $5.91 \text{ g}_w/\text{g}_{\text{dry matter}}$ and when it finished, the moisture content of the dried grapes reached a final level of $0.15 \text{ g}_w/\text{g}_{\text{dry matter}}$. Moreover, every single experiment was repeated three consecutive times, and then the obtained results were averaged.

2.3. Measuring Instruments

The meteorological parameters as well as the temperature, humidity and velocity of air during the solar drying process were measured to evaluate the performance of SGD under different operational conditions. Temperatures of the enclosure of SGD and woven mesh were measured using K-type thermocouples. Temperatures, the velocity of outlet hot air of SAH (in the case of forced convection mode) and output humid air from SGD were recorded using a velocity meter, while the solar irradiance was measured using a solar power meter. The relative humidity of ambient air and drying air (air in the enclosure of SGD) were measured as well. The range, resolution and accuracy of the measuring equipment are shown in Table 4.

Table 4. Description of the measuring equipment.

Parameter	Equipment	Measuring Range	Resolution	Accuracy
Temperature	Digital thermometer, 4 channels (TENMARS, TM747DU, Taiwan)	-100 – $+1300$ °C for K-type	0.1 °C	$\pm 0.1\%$ rdg $+0.7$ °C
Temperature and relative humidity (RH) of ambient air	Digital temperature–humidity meter with probe (Pro’sKit NT-312, Taiwan)	Temperature: -50 – $+70$ °C RH: 20–90%	0.10 °C 1% RH	$\pm 1\%$ °C $\pm 5\%$ RH
Solar radiation intensity (pyranometer)	Digital data logging solar power meter (TENMARS, TES-132, Taiwan)	0–2000 W/m ²	1 W/m ²	± 10 W/m ²
Air velocity (anemometer)	Digital hot-wire air velocity meter and probe (TENMARS, TM-4002, Taiwan)	0.01–25 m/s	0.01 m/s	$\pm 3\%$ rdg, $\pm 1.6\%$ FS
Weight of grape sample	Digital electronic balance (WANT WT-N, China)	Up to 5000 g	0.10 g	± 2 d at max capacity

2.4. Solar Drying Modes

The solar drying process of grapes using the glass and Plexiglas SGDs was carried out with the three drying modes described below:

2.4.1. Natural Convection Mode for SGD (CN-SGD)

This mode is considered the simplest and cheapest method for drying agro-products using SGD. In this mode (Figure 4a), the SGD was provided with one circular port (8 cm in diameter) as an inlet for ambient air, which was drilled at the bottom edge of the wall of SGD that faced the wind direction in the experimental location. Meanwhile, the humid air vent (square port 8 cm × 8 cm) was located in the opposite top roof of the SGD to increase the buoyancy force, which helps in creating an air draft inside the enclosure of SGD.

2.4.2. Forced Convection Mode for SGD (FC-SGD)

In this mode, three speeds of the centrifugal fan of SAH were used to provide the SGD with different airflow rates (Figure 4b). A voltage regulator set the voltage outside the PV panel to a maximum of 12 volts to suit the consumption of the fan. Then, a dimmer (speed regulator) switch was used to change the voltage. Consequently, the fan speed was set to 12, 9 and 5 V to obtain outlet hot air with mass flow rates of 0.06, 0.04 and 0.03 kg/s, respectively, from SAH.

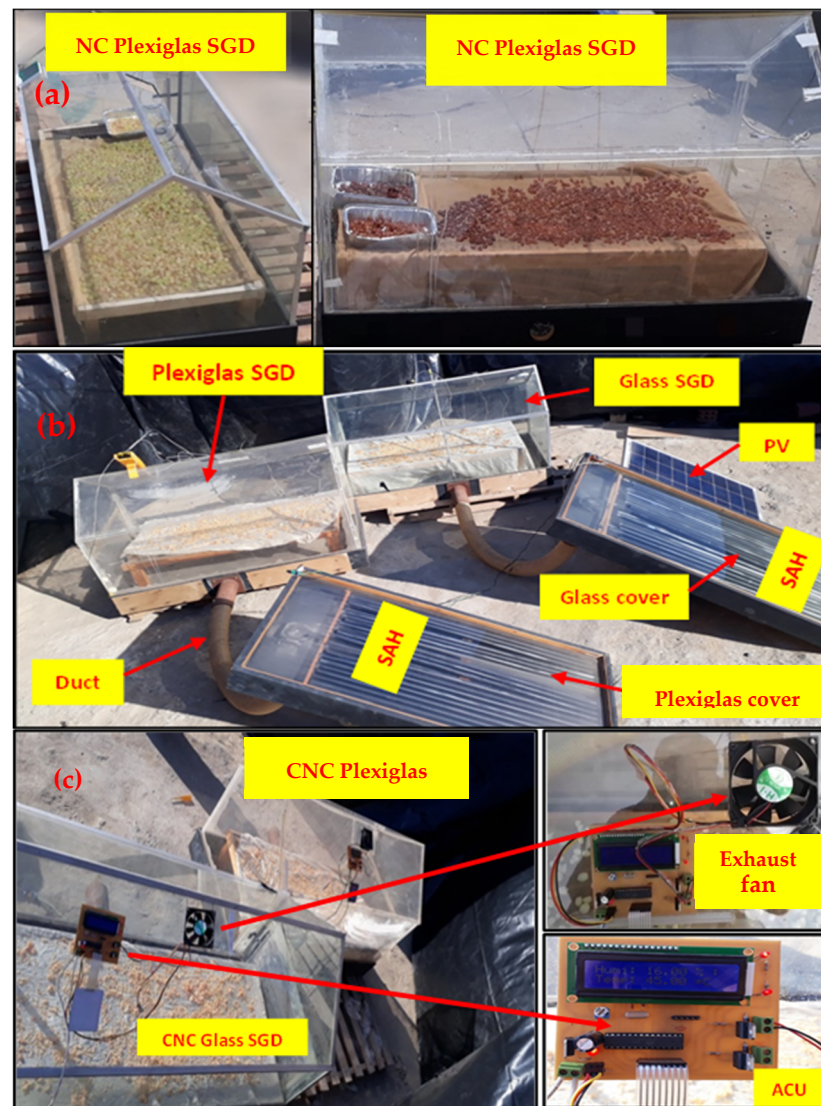


Figure 4. The designs of SGD for drying grapes: (a) natural convection (NC) mode, (b) forced convection (FC) mode, (c) controlled natural convection (CNC) mode (new mode).

2.4.3. Controlled Natural Convection Mode for SGD/New Mode (CNC-SGD)

Regarding the new mode, a similar SGD to that used in the conventional natural mode was equipped with a fan (DC 12 Volts/0.25 A) that acted as an exhaust air fan to vacuum an ambient air stream with a constant velocity of 2 m/s across the enclosure of the SGD. The exhaust air (humid air) fan was installed on the top roof of the SGD exactly on the humid air vent and connected to the automatic control unit (Figure 4c). The ACU operated the fan when it was essential to change the temperature and relative humidity values rather than the automatic pre-adjusted values. Thus, the intermittent operation of the exhausted air vacuum fan precisely preserved the temperature and relative humidity of the drying air inside the SGD.

2.5. Calculations and Determinations

2.5.1. Thermal Efficiency of SAH

The thermal efficiency of the used SAH is defined as the accumulated useful energy extracted from the solar collector throughout the experimental time divided by the total solar radiation incident on the collector. The thermal efficiency of the SAH (η_c) can be determined using the equation given by Sexina et al. [59]:

$$\eta_c = \frac{\dot{m}_a \times C p_a (T_{co} - T_{ci})}{I_c \times A_c} \times 100 \quad (1)$$

where \dot{m}_a , $C p_a$, T_{co} , T_{ci} , I_c and A_c are, respectively, the mass flow rate of air (kg/s), specific heat of air (J/kg K), outlet temperature of the solar air heater ($^{\circ}\text{C}$), inlet temperature of the solar air heater ($^{\circ}\text{C}$), total incident solar radiation intensity on the solar air heater (W/m^2) and surface area of the solar air heater/collector (m^2).

2.5.2. Drying Kinetics

The moisture content (M) on the dry basis, moisture ratio (MR) and drying rate (DR) can be determined using Equations (2)–(5) as follows:

$$M = \frac{m_p - m_d}{m_d} \quad (2)$$

$$MR_{exp} = \frac{M_t - M_e}{M_0 - M_e} \quad (3)$$

where m_p , m_d , M_0 , M_e and M_t are, respectively, the mass of the product, the corresponding dry matter, the initial moisture content, the moisture content in the equilibrium state and the moisture content at moment t .

Nevertheless, because M_e is very small compared to M_t and M_0 , MR is simplified according to [60,61] as:

$$MR_{exp} = M_t / M_0 \quad (4)$$

where MR_{exp} is the experimental moisture ratio. The drying rate (DR) is estimated on the basis of the ratio of the difference in two consecutive values of M_t and time difference (Δt), as given by [62]:

$$DR = \frac{M_{t+\Delta t} - M_t}{t} \quad (5)$$

The experimental values of MR_{exp} for the three drying modes used in the present study were fitted to the following five thin drying mathematical models: the Lewis model: $MR = \exp(-\hat{k}t)$ [63], Page model: $MR = \exp(-\hat{k}t^n)$ [64], Henderson and Pabis model: $MR = \hat{a} \exp(-\hat{k}t)$ [65], Wang and Singh model: $MR = 1 + \hat{a}t + \hat{b}t^2$ [66] and parabolic model: $MR = \hat{a} + \hat{b}t + \hat{c}t^2$ [67]. To compare the fitness of the mentioned drying models in order to select the proper model that describes the behavior of the drying process of the product for generalizing the drying curve [68], values of the coefficient of determination (R^2), chi-squared (X^2) and root mean square error ($RMSE$) were estimated using the equations below [69,70]:

$$R^2 = 1 - \frac{\sum_{i=1}^N (MR_{pre,i} - MR_{exp,i})^2}{\sum_{i=1}^N (MR_{exp,i})^2} \quad (6)$$

$$X^2 = 1 - \frac{\sum_{i=1}^n (MR_{exp,i} - MR_{pre,i})^2}{N - n} \quad (7)$$

$$RMSE = \sqrt{\frac{\sum_{i=1}^n (MR_{exp,i} - MR_{pre,i})^2}{N}} \quad (8)$$

where n , N , MR_{exp} and MR_{pre} are, respectively, the total number of observations, number of constants, experimental moisture ratio, % (wb), and predicted moisture ratio, % (wb).

2.5.3. Performance of the Dryer

The drying thermal efficiency (η_d) of the SGD can be calculated using the following equation [71]:

$$\eta_d = \frac{(M_i - M_b) \times h_l}{(A_d \times I_v \times D_b)} \times 100 \quad (9)$$

where M_i, M_b, h_l, A_d, I_v and D_b are, respectively, the initial mass of one batch of grapes (kg), mass of dried grapes from one batch (kg), latent heat of vaporization (kJ/kg), area of dryer (m^2), average incident solar radiation intensity on dryer (W/m^2) and time taken for drying one batch of grapes sample.

2.6. Economic Assessment

In the present study, the economic analysis was performed based on the fact that SGDs are used only during the warmer months of the year. This assessment was mainly based on the cost in the country in which the present study was performed. Therefore, the annual production in the present analysis will be estimated for the warmer period in Egypt from May to September. The cost of SGD based on the cover material and operating modes is tabulated (Table 5).

Table 5. Cost of the SGD’s components (USD) with different drying modes using two types of covering materials.

Component	No. of Pieces	Cost (USD)	Notes
Plexiglas SGD	1	40	-
Glass SGD	1	37	-
Plexiglas SAH	1	35	For Plexiglas FC mode only
Glass SAH	1	32	For Glass FC mode only
Air duct	2	10	For Glass and Plexiglas FC modes
PV panel	1	25	For Glass and Plexiglas FC and CNC modes
Voltage regulator, dimmer and wires	2	10	For Glass and Plexiglas FC modes
ACU and exhaust fan	2	10	For Glass and Plexiglas CNC modes
Wooden platform	2	25	For Glass and Plexiglas CN modes
Assembly cost	-	24	For all designs
Total cost	NC-SGD	USD 86 (Glass)	USD 89 (Plexiglas)
	FC-SGD	USD 148 (Glass)	USD 154 (Plexiglas)
	CNC-SGD	USD 106 (Glass)	USD 109 (Plexiglas)

The drying cost per mass unit of grapes (USD/kg) by using the annualized cost method was performed for an economic evaluation of SGD with the three operating modes using the glass SGD and Plexiglas SGD. The lifespan (j) of the used SGD, SAH and PV panel was taken as 10 years [72]. The annualized cost (C_a) can be calculated using equations adopted from [73]:

$$C_a = C_{ac} + C_{O\&M} - S_a + C_{re} \tag{10}$$

Since SGDs are used on the domestic scale, the running cost (C_{re}), which is represented in the annual labor daily wage for operating the dryer, will be ignored. The number of days using the dryer per year will be 120 days (hottest period of the year from May to August).

C_{ac} is the annualized capital cost, which can be calculated using equation the below:

$$C_{ac} = C_{CC} \times CRF \tag{11}$$

where C_{cc} is the capital cost of the dryer (USD) and CRF is the capital recovery factor that can be estimated as:

$$CRF = \frac{i(1+i)^j}{(1+i)^j - 1} \tag{12}$$

where i is the discount rate, which is 9.25% (Central Bank of Egypt, 2021) and j is the life span of the drying system (assumed to be 10 years).

The annual operating and maintenance cost ($C_{O\&M}$) is taken as 6% of annualized capital cost (C_{ac}) as:

$$C_{O\&M} = 0.06 \times C_{ac} \tag{13}$$

The annualized salvage value (S_a) is calculated as:

$$S_a = S \times SFF \quad (14)$$

where S is the salvage value taken as 10% of the annual capital cost (C_{ac}) of the dryer [30] and SFF is the sinking fund factor, which can be estimated as:

$$SFF = \frac{i}{(1+i)^j - 1} \quad (15)$$

Thus, the drying cost per 1 kg of dried grapes (C_d) is determined using the following relation:

$$C_d = \frac{C_a}{P} \quad (16)$$

where P is the annual mass of dried grapes (kg/year) produced by the dryer and can be estimated as:

$$P = \frac{M_b \times D}{D_b} \quad (17)$$

To calculate the money saving for the dryer across its life, the saving per day for the base year for the dryer (S_{db}) can be calculated using Equations (16) and (17) [53]:

$$C_{ds} = C_{fp} \times \frac{M_i}{M_b} + C_d \quad (18)$$

$$S_{db} = \frac{(C_{mr} - C_{ds})}{D_b} \quad (19)$$

where C_{mr} is the price of 1 kg of dried grapes (raisins) in the local market (USD 9).

Then, the total savings (S_j) for the dryer after (j) number of years can be calculated as given by [68]:

$$S_j = S_{db} \times D \times (1+i)^{j-1} \quad (20)$$

The payback period (N_p) is determined using the following equation [68]:

$$N_p = \frac{\ln\left(1 - \frac{C_{cc}}{S_1}(i-d)\right)}{\ln\left(\frac{1+d}{1+i}\right)} \quad (21)$$

Note: d is the inflation rate (5.21 %, The Central Bank of Egypt, 2021).

3. Results and Discussions

3.1. Fluctuation in Solar Radiation Intensity (SRI)

Figure 5 shows the variation in the total incident solar radiation intensity (SRI) on the horizontal plane during the drying period of 8 to 16 h on each experimentation day. The variation in SRI is shown for outside the SGD, inside the glass and in the Plexiglas with the different drying modes. The SRI increased gradually before noon to reach its peak value at noon from 12 to 12:30 pm on each typical day. Since the drying process is accomplished chiefly over two days, at least for the high-moisture content products, the average SRI of two consecutive days for each drying mode using the glass and Plexiglas SGDs was recorded. The average SRI outside and in the Plexiglas SGD during the drying period (8 h/day) was 745.22, 753.33 and 744.94 W/m² for the experimental days of NC-SGD, FC-SGD and CNC-SGD, respectively, while the average SRI inside the glass SGD was 663.99, 673.83 and 658.95 W/m², and in the Plexiglas SGD, it was 630.42, 636.79 and 628.31 W/m² for the same mentioned modes, respectively. The data show that the transmissivity of glass and Plexiglas are about 89 and 85%, respectively.

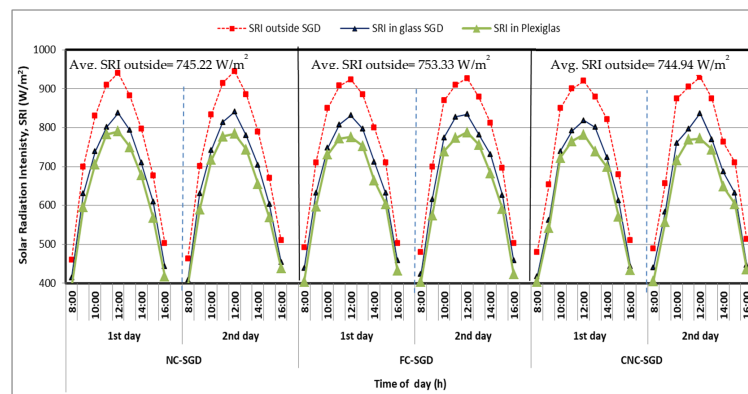


Figure 5. Changes in incident SRI in glass and Plexiglas SGDs during typical experimentation days with different drying modes.

3.2. Thermal Performance of SAHs (for FC Drying Mode)

The SAHs were tested under three different air mass flow rates (\dot{m}_a), 0.03, 0.04 and 0.06 kg/s, through a set of preliminary outdoor experiments to determine the most suitable air flow rate for the forced convection drying mode. The obtained results showed that the maximum achievable temperature for the hot air was achieved by using the air mass flow rate of 0.03 kg/s. As illustrated in Figure 6a, the maximum and average incident solar radiation intensity on the plane surface (I_c) of the SAHs was 940 and 789.7 W/m², respectively. In the present study, the ambient temperature was considered as the inlet air temperature (T_{ci}) for both SAHs, with the glass and Plexiglas covers. The inlet air temperature was measured and found to be in the range of 32.8–41.1 °C during the typical day drying period from 8 to 16 h, while the outlet air temperature (T_{co}) ranged from 36 to 61 °C and from 36.8 to 62.1 °C for the SAH with the glass and Plexiglas cover, respectively.

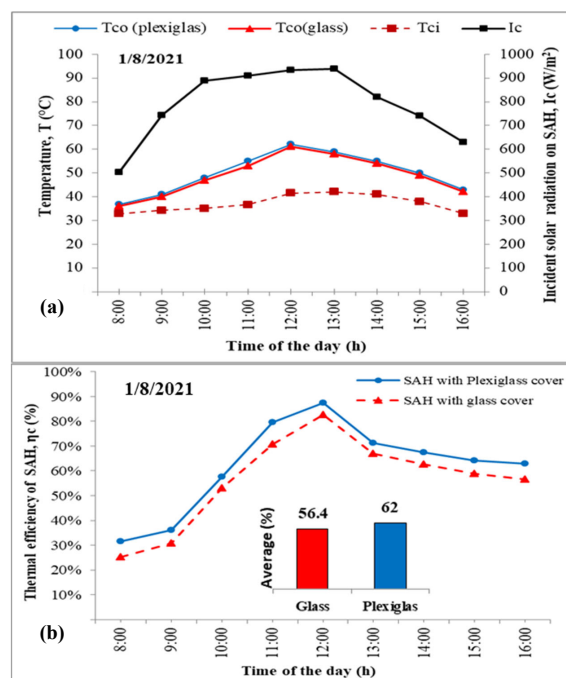


Figure 6. Thermal performance of SAH at a air mass flow rate of 0.03 kg/s. (a) Variation in solar radiation and temperatures of SAH; (b) thermal efficiency of SAH.

Figure 6b shows that the thermal efficiency (η_c) of the SAHs throughout the daily drying period using an air mass flow rate of 0.03 kg/s reached its maximum value at noon (12 h). Afterwards, it started to reduce gradually, although the solar radiation intensity

increased, reaching its peak value at 12:30 h. This can be attributed to thermal losses. The average thermal efficiency was found to be 56.40 and 62% for the SAH covered with glass and Plexiglas, respectively. Hence, it is clear that the SAH with the Plexiglas cover showed a better thermal performance compared to the same SAH covered by glass. In summary, the Plexiglas SAH showed higher thermal efficiency than the glass SAH by about 9% at $\dot{m}_a = 0.03 \text{ kg/s}$.

3.3. Variation in Temperature and Relative Humidity of Ambient Air and Across SGD

Figure 7 illustrates the variation in the temperatures of ambient air (T_a) and drying air inside the glass dryer (T_g) and inside the Plexiglas dryer (T_p), as well as the relative humidity of ambient air (RH_a) and humid air inside both the glass dryer (RH_g) and Plexiglas dryer (RH_p). The ranges of the measured temperature and relative humidity for the ambient air were 30–41.40 °C and 40–65% for the natural convection drying mode, while these values were 30.50–41 °C and 42–69% for the forced convection drying mode and 31.3–39.3 °C, 27–64% for the new controlled natural convection drying mode. As a general pattern, the ambient temperature had an opposite trend to the ambient relative humidity till around noon, wherein the ambient temperature in the first hour of the drying period (8 h) was low, while the ambient relative humidity was at a high level, as shown in Figure 7. This pattern continued till 14 h, and then both the ambient temperature and relative humidity decreased. Afterwards, the ambient relative humidity began to increase slightly in the last hour of the drying period (16 h), while the ambient temperature continued to decrease. The obtained ranges of the temperature and relative humidity inside the Plexiglas SGD were found to be 38–52.3 °C and 26–54% for NC-SGD, 45–59 °C and 17–36% for FC-SGD and 42–55.6 °C and 20.4–42% for CNC-SGD. On the other hand, these ranges for the glass SGD were 38–50 °C and 29–52% for NC-SGD, 43–55 °C and 19–39% for FC-SGD and 41.3–55.3 °C and 19–41.3% for CNC-SGD. It should be noted that the highest average temperature for the interior air inside the Plexiglas SGD was 53 °C for FC-SGD, followed by 50.40 °C for CNC-SGD, and the lowest temperature was 46.50 °C for NC-SGD, while inside the glass dryer, the temperatures were 51.20, 50.20 and 44.70 °C for the mentioned modes, respectively. FC-SGD had the highest achieved temperature inside both the Plexiglas and glass dryers under all drying modes due to the vital role of SAH in providing the dryer with an adequate hot air stream. Meanwhile, the new drying mode of CNC showed higher temperatures across the enclosure of the dryer compared to the conventional natural convection drying mode, which were very close to the temperatures inside the FC-SGD whether the dryer was covered with glass or Plexiglas. This occurred despite the fact that the CNC-SGD did not have an auxiliary heating tool (e.g., SAH).

Concerning the relative humidity across the enclosure of dryer, the results showed that the average relative humidity of interior air inside the Plexiglas SGD was found to be 24.80, 25.1 and 35.40% for FC-SGD, CNC-SGD and NC-SGD, respectively, while these averages inside the glass SGD were 24.8, 25.70 and 35.7% for the drying modes mentioned above, respectively. It was observed that CNC-SGD achieved approximately equal values for the relative humidity inside both the glass and Plexiglas dryers. These values were found to be very close to values achieved by the FC drying mode, and the relative humidity was lower than the NC drying mode by about ~10%.

Since higher temperature ranges and lower ranges of relative humidity inside the dryer lead to quick moisture removal, as reported by Badaoui et al. [69], thus, the new mode (CNC) achieved a high difference between the temperature and relative humidity of drying air inside the Plexiglas and glass SGDs, like the FC drying mode. This means that the CNC mode can enhance the drying efficiency and shorten the drying time and can be used for drying products with high moisture content instead of the slow NC drying system or even the high-cost FC drying system.

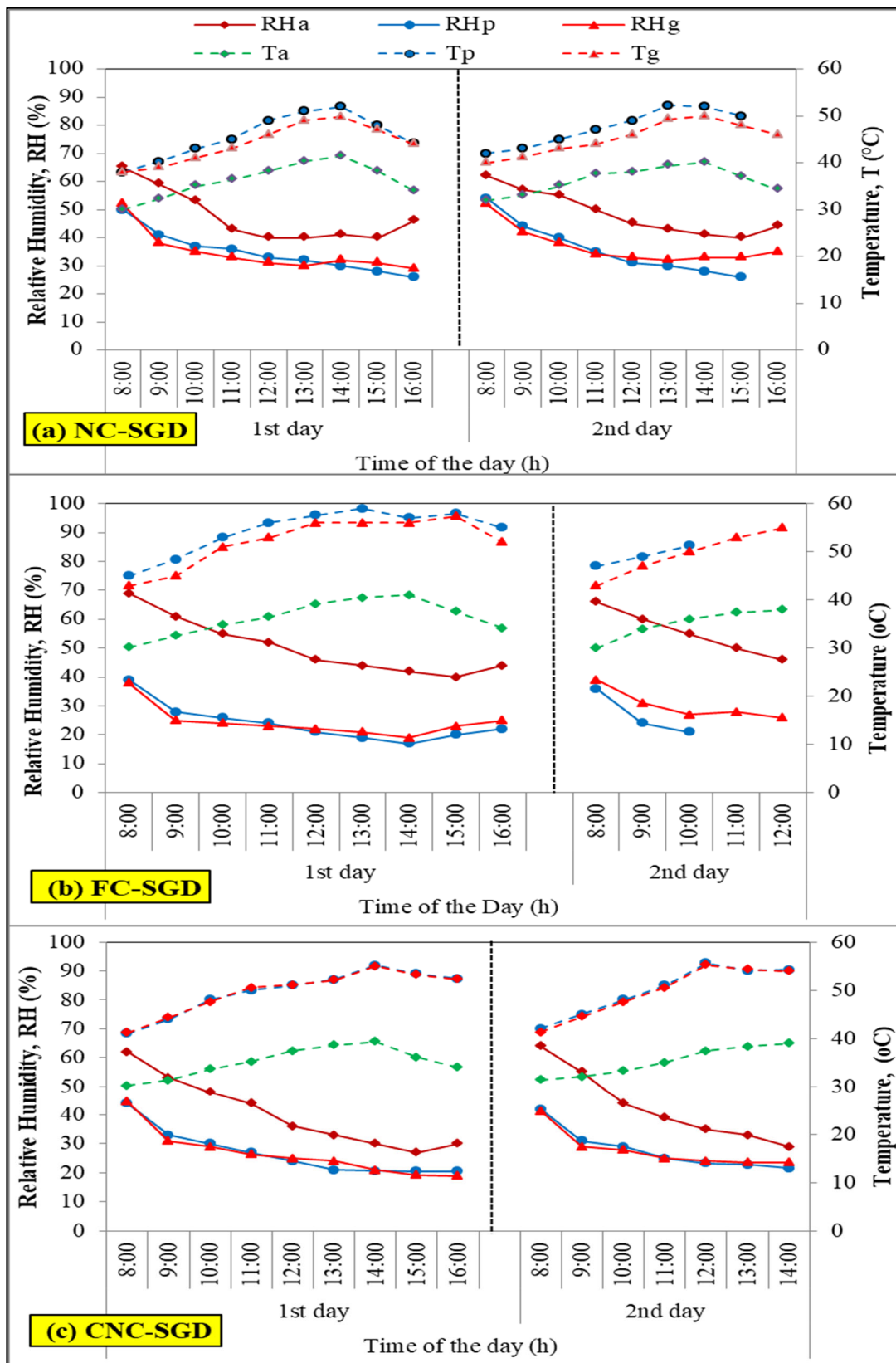


Figure 7. Variation in temperatures and relative humidity of air across the glass and Plexiglas SGDs in drying modes (a) NC, (b) FC ($m_a = 0.03 \text{ kg/s}$) and (c) CNC.

3.4. Variation in Moisture Content, Drying Rate and Moisture Ratio during Grape Drying

Figure 8a depicts the variation in the grapes' moisture content throughout the drying period, which was extended to two consecutive days for each drying experiment using Plexiglas and glass SGDs with the different drying modes. As a general pattern, it was noticed that the moisture content removal rate was quite slow in the first 3 h of the drying process, which can be attributed to the high relative humidity and low temperature of the drying air inside the SGD at the beginning of the drying process. Afterwards, it declined continuously with the drying time without a constant-rate drying period, which was in agreement with the results given by El Khadraoui et al. [31], accompanied by a low drying rate at end of the drying process (i.e., the second day).

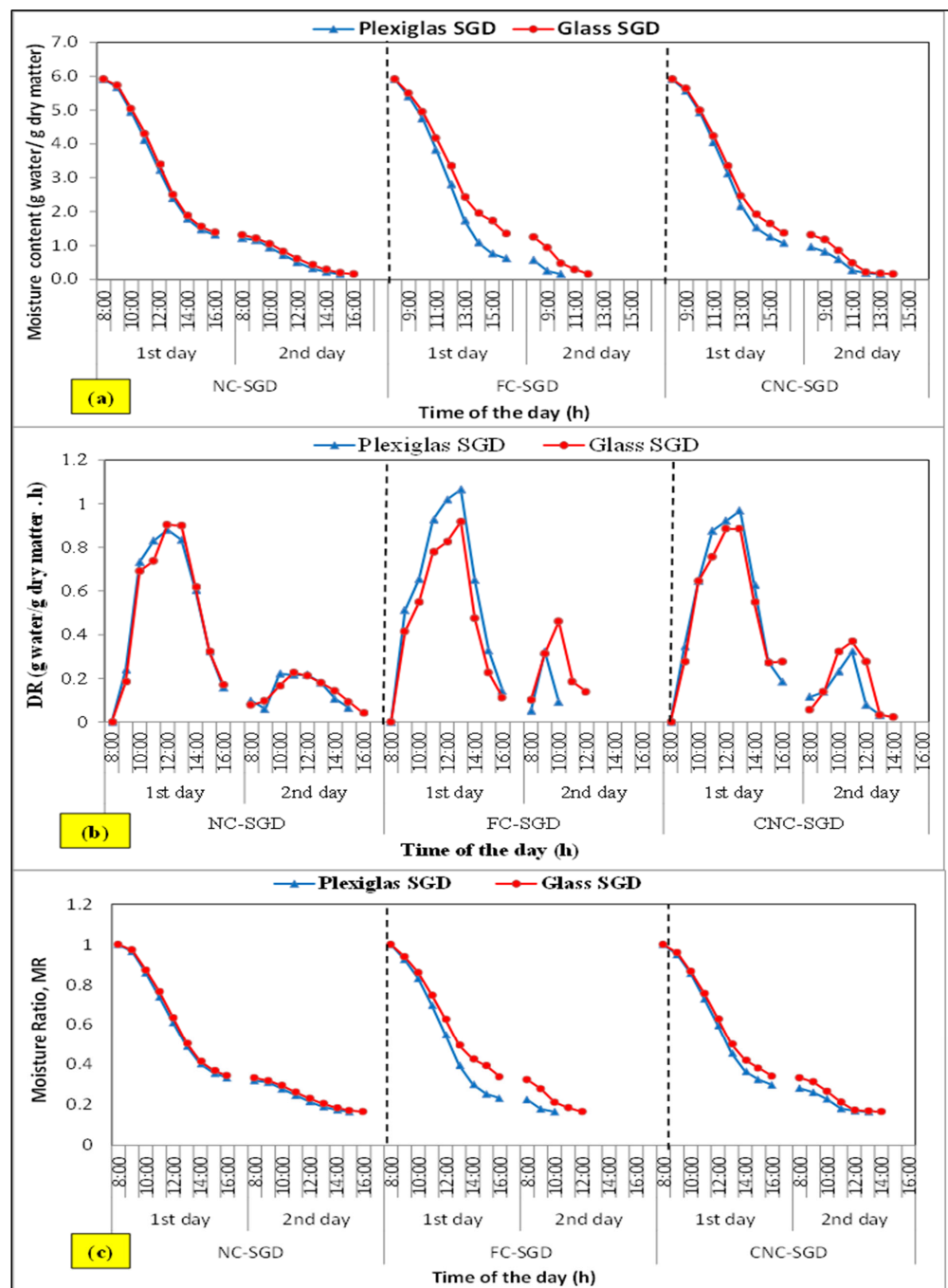


Figure 8. Drying behavior of the Plexiglas and glass SGD with different drying modes: (a) moisture content, (b) drying rate, (c) moisture ratio.

In the case of the glass SGD, the obtained results showed that the initial moisture content of grapes on the dry basis of 5.91 (g water/g dry matter) was reduced to the final moisture content of 0.15 (g water/g dry matter) in 16, 12 and 13 h (see the drying time in Figure 9) by using the three drying modes of NC, FC and CNC, respectively (Figure 8a), whereas the initial moisture content of grapes was reduced inside the Plexiglas SGD to the same final moisture content in about 15, 10 and 12 h by using the three mentioned drying modes, respectively.

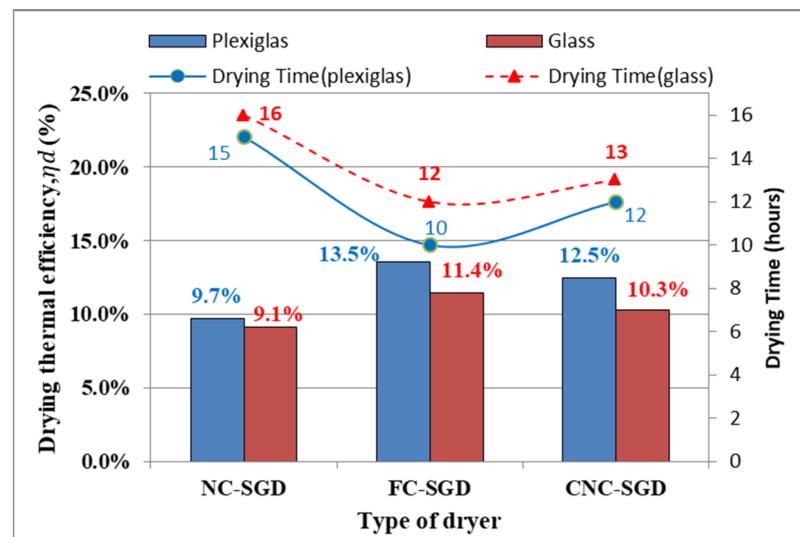


Figure 9. The overall drying thermal efficiency and drying time of the Plexiglas and glass SGDs with different drying modes.

The drying rate of the grapes against the drying time is depicted in Figure 8b. As a general trend for the three drying modes, a rapid drying rate is observed till the peak point around noon. Afterwards, it decreased to reach the lowest rate in the last hour of the drying time without a constant drying period, which is in agreement with El Khadraoui et al. [31] and Hamdi et al. [52]. This is because the drying process in the falling down process is controlled by the internal water diffusion from the interior of the grape to the surface, which is in agreement with Akpınar [74]. The drying rate of CNC-SGD is higher than NC-SGD and very close to the highest rate of FC-SGD, although CNC-SGD had no extra heating device like the FC drying mode did. Thus, the new drying mode of CNC, whether covered by glass or Plexiglas, is considered a potential feature represented in the full control of the recommended temperature and relative humidity inside the dryer throughout the entire period of drying.

The variation in the moisture ratio during the practical experiments (MR_{exp}) for the three drying modes, NC, FC and CNC, vs. the drying time in typical days of the experiment is shown in Figure 8c. Figure 8c depicts that the moisture ratio of the grapes during the drying process has the same trend as that of the moisture content with the three drying modes. The curves of the experimental MR_{exp} were regressed to five thin-layer drying models, which will be discussed in detail in the upcoming Section 3.5, to identify the best model that achieves the lowest difference between the experimental and predicted MR values.

Figure 9 shows the overall drying thermal efficiency (η_d) for the three drying modes, NC, FC and CNC. The FC drying mode had the highest efficiency of 11.4 and 13.5% for glass and Plexiglas SGDs, respectively. This may be due to the significant effect of SAH, besides the heat of direct irradiance, which leads to a rapid drying rate. Meanwhile, the new drying mode CNC also achieved a rapid drying rate of 10.3 and 12.5% for glass and Plexiglas SGDs, respectively, without any additional heating device, whereas the NC drying

mode had the lowest efficiencies of 9.1 and 9.7% for the two types of glass and Plexiglas SGDs, respectively.

It is clear that the CNC drying mode shows better performance for drying high-moisture products such as grapes compared to the NC drying mode, while it can also be used as a good alternative to the complicated FC drying system, which has the SAH and the other components that require more occupation area and high initial and operating costs.

3.5. The Mathematical Thin-Layer Drying Model for Grapes

Five mathematical thin-layer drying models were fitted to experimental values of the moisture ratio to find out the best model able to describe the behavior of the drying process of the Sultana grapes with the three drying modes, NC, FC and CNC, whether the dryer was covered by glass or Plexiglas, as shown in Figure 10. The evaluation of the performance of the used empirical equations of the thin layer models was carried out using three statistical indicators: the coefficient of determination (R^2), chi-squared (χ^2) and root mean square error (RMSE). The constants of models and values of statistical indicators are shown in Table 6. From the obtained data, it is clear that the equation of the Page model is considered the best fitting equation to describe the thin-layer drying process of Sultana grapes with all drying modes of NC, FC and CNC, whether in case of using glass or Plexiglas as the covering material, as depicted in Figure 10 and Table 6 in bold font. Concerning the new drying mode of CNC, Table 6 shows a good agreement between the experimental values of the moisture ratio and the predicted ones, where statistical criteria values for the Plexiglas SGD were $R^2 = 0.9775$, $\chi^2 = 0.006$ and $RMSE = 0.0242$, but for the glass SGD, they were $R^2 = 0.9716$, $\chi^2 = 0.0010$ and $RMSE = 0.0299$.

Table 6. The constants of the different thin-layer models and the statistical indicators for drying grapes using the glass and Plexiglas SGDs.

Drying Mode	Model Name	Type of Cover	Constants					R^2	χ^2	RMSE
			k	n	a	b	c			
NC-SGD	Lewis	Plexiglas	0.1405					0.7237	0.0741	0.2640
		glass	0.1375					0.7000	0.0686	0.2545
	Page	Plexiglas	0.4015	0.9702				0.9479	0.0018	0.0395
		glass	0.3496	1.0102				0.9373	0.0022	0.0443
	Wang and Singh	Plexiglas			-0.162	0.0074		0.8810	0.0517	0.2063
		glass			-0.178	0.0086		0.9068	0.0488	0.2016
	Henderson and Pabis	Plexiglas	0.3200		0.6780			0.9665	0.0129	0.1068
		glass	0.3060		0.6828			0.9669	0.0134	0.1092
	Parabolic	Plexiglas			0.8193	-0.1618	0.0074	0.8810	0.0116	0.0976
		glass			0.8686	-0.1784	0.0086	0.9068	0.0183	0.1236
FC-SGD	Lewis	Plexiglas	0.2010					0.8614	0.0660	0.2450
		glass	0.1747					0.8561	0.0596	0.2346
	Page	Plexiglas	0.5200	1.0030				0.9926	0.0001	0.0094
		glass	0.4525	0.9555				0.9893	0.0002	0.0147
	Wang and Singh	Plexiglas			-0.235	0.0150		0.9450	0.0309	0.1523
		glass			-0.193	0.0104		0.9311	0.0372	0.1709
	Henderson and Pabis	Plexiglas	0.5010		0.8977			0.9871	0.0016	0.0386
		glass	0.3900		0.8944			0.9822	0.0014	0.0364
	Parabolic	Plexiglas			0.8654	-0.2351	0.0150	0.9450	0.0059	0.0730
		glass			0.8475	-0.1926	0.0104	0.9311	0.0066	0.0780
CNC-SGD	Lewis	Plexiglas	0.1643					0.7933	0.0691	0.2533
		glass	0.1579					0.7874	0.0626	0.2418
	Page	Plexiglas	0.4425	0.9854				0.9775	0.0006	0.0242
		glass	0.3886	1.0030				0.9716	0.0010	0.0299
	Wang and Singh	Plexiglas			-0.186	0.0096		0.9142	0.0421	0.1835
		glass			-0.172	0.0082		0.9073	0.0397	0.1797
	Henderson and Pabis	Plexiglas	0.3880		0.7786			0.9779	0.0065	0.0779
		glass	0.3620		0.8321			0.9758	0.0044	0.0644
	Parabolic	Plexiglas			0.8390	-0.1860	0.0096	0.9142	0.0082	0.0873
		glass			0.8392	-0.1722	0.0082	0.9073	0.0087	0.0901

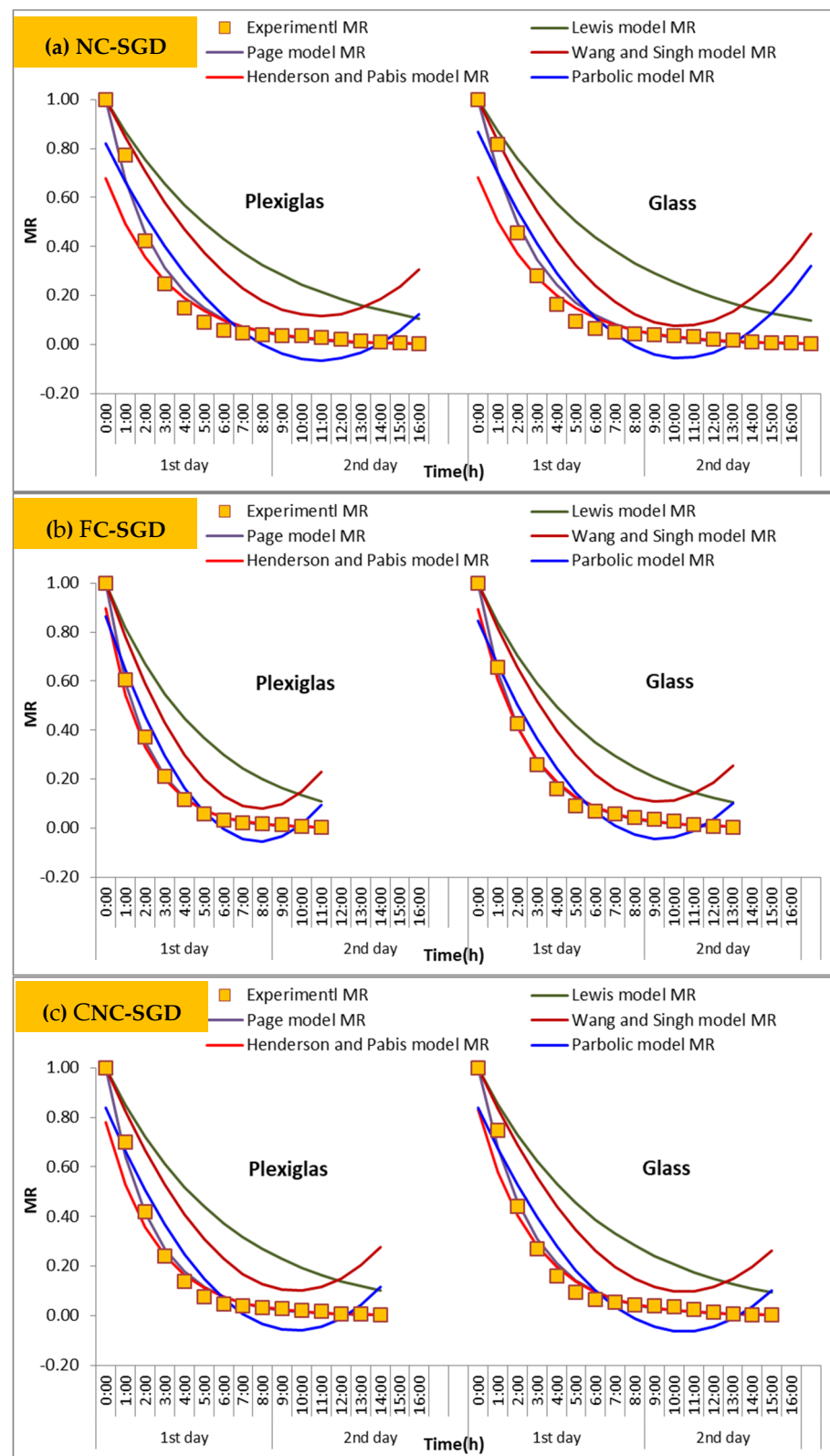


Figure 10. The variation in the experimental and predicted MR versus the drying time using glass and Plexiglas SGDs with the different drying modes.

3.6. Economic Assessment

The economic assessment was performed for the Plexiglas and glass SGDs with the three drying modes of NC, FC and CNC to obtain deep insights into the best operational

mode of an SGD suitable for domestic/small-scale drying purposes from an economic perspective. The economic assessment was carried out in terms of the criterion cost of 1 kg of the dried grapes/solar-dried raisins (C_d), the total saved cost over the lifespan of the dryer (S_j) and the payback period (N_p) to recover the invested costs. From Figure 11a–c, it can be observed that the Plexiglas SGD achieved better results for the economic parameters with all drying modes compared to the glass SGD.

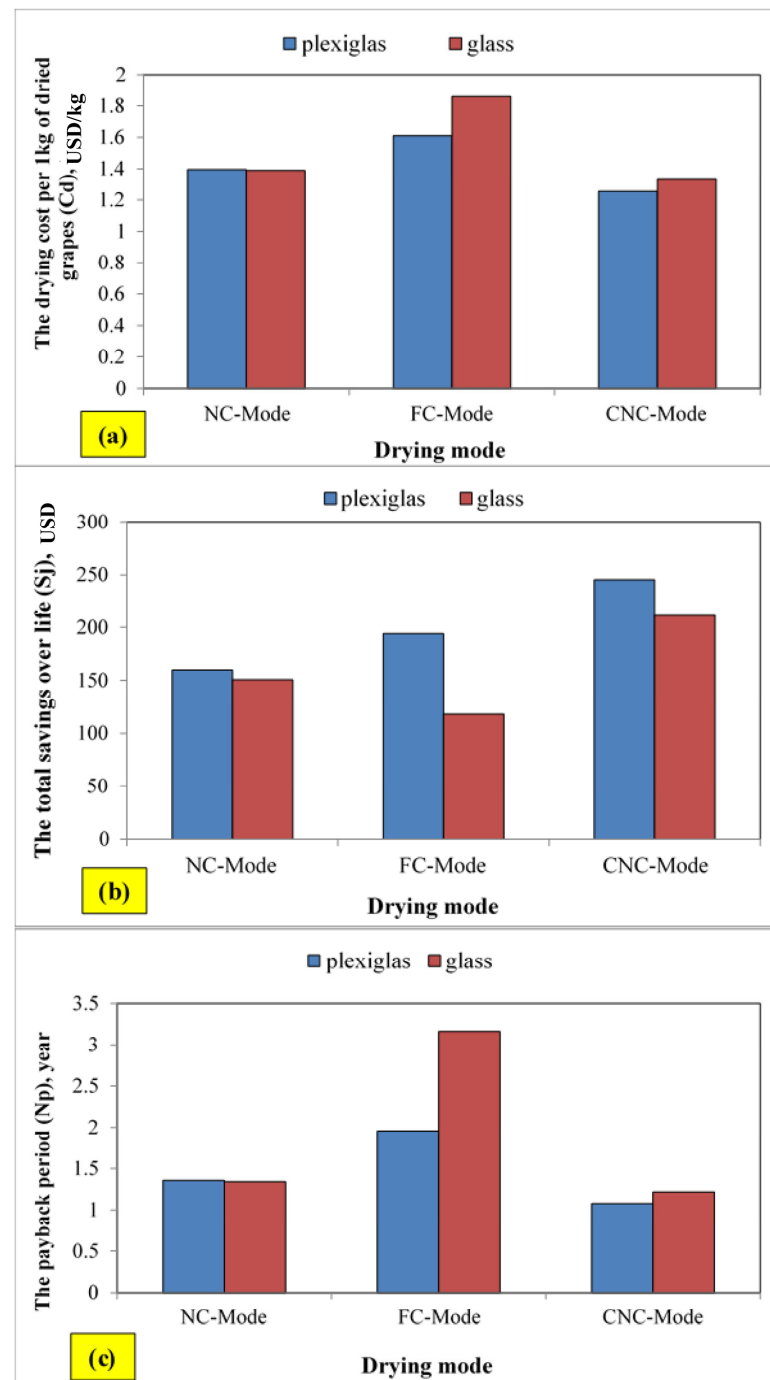


Figure 11. Economic assessment of Plexiglas and glass SGDs with different drying modes: (a) drying cost per unit of mass of dried grapes, (b) total saving cost, (c) payback period.

The calculations of the economic assessment revealed that the glass SGD using the FC drying mode had the highest value of C_d (1.86 USD/kg), low S_j (USD 117.96) and the longest N_p (3.16 years) compared to the other two drying modes. This can be attributed

to the heating auxiliary collector (SAH), in addition to its fittings and the photovoltaic (PV) system. Although the CNC-SGD was operated using a PV system like FC-SGD, the lowest value of C_d (1.26 USD/kg), the highest value of S_j (USD 245.46) and the shortest N_p (1.08 year) were achieved in case of using the Plexiglas CNC-SGD.

Despite the fact that the NC-SGD has lower initial, operating and maintenance costs than the two other dryers, FC-SGD and the new CNC-SGD, whether using the glass or Plexiglas cover, it has lower thermal performance and a slow drying rate because it depends completely on the fluctuating direction and velocity of the ambient air.

It is clear that the development and conversion of conventional NC-SGD to the new fully controlled natural convection drying mode (CNC) gave the advantage to this new mode of controlling the pre-adjusted recommended temperature and humidity inside the SGD continuously throughout the entire drying period daily (8 h). This led to more evaporation of water from grapes at a uniform and quick rate and, consequently, a productivity and drying time higher and shorter, respectively, than the NC drying mode and slightly lower than the FC mode, particularly by using the Plexiglas SGD due to its ability to conserve the accumulated heat inside the dryer for a longer time. Moreover, the new drying mode of CNC is not augmented with a heating device, which reduces the initial cost, and leads to a lower C_d , higher S_j and shorter N_p than the FC mode.

4. Conclusions

The present study proposed a new drying mode named controlled natural convection (CNC) for drying grapes (Sultana variety) as a high-moisture content agro-product using a direct solar greenhouse dryer (SGD) with two types of cover material, glass and Plexiglas. The thermal performance of the new drying mode using a solar greenhouse dryer (CNC-SGD) was investigated to be used as a potential alternative for the conventional natural convection solar greenhouse dryer (NC-SGD), which is featured as a slow drying mode, and also compared to the expensive and complicated forced convection solar greenhouse dryer (FC-SGD). CNC-SGD was provided with an automatic control unit operated by a PV system to assure full control of the operating conditions inside the dryer. In general, the obtained results revealed that the Plexiglas SGD showed better results compared to the glass SGD under all operating conditions. In the case of the CNC mode using the Plexiglas SGD, the obtained results showed that the initial moisture content of grapes on the dry basis of 5.91 g water/g dry matter was reduced to a final moisture content of 0.15 g water/g dry matter in about 12 h with a thermal drying efficiency of 12.5%, which is very close to the FC drying mode (10 h and 13.5%) and higher than the NC drying mode (15 h and 9.7%).

The Page model was found to be the most appropriate mathematical model to describe the behavior of the drying process of the NC, FC and CNC modes whether with the Plexiglas SGD or glass SGD. A good agreement between the experimental and predicted MR values was found in the new CNC mode using the Plexiglas SGD, as $R^2 = 0.9775$, $\chi^2 = 0.0006$ and RMSE = 0.0242.

Concerning the economic assessment, the new CNC drying mode using the Plexiglas SGD has the lowest cost per 1 kg of dried grapes (1.26 USD/kg), the highest saved costs over the lifespan of the dryer (USD 245.46) and the shortest payback period (1.08 year), whilst the highest cost per 1 kg of dried grapes (1.86 USD/kg), the lowest saved costs (USD 117.96), and the longest payback period (3.16 years) was recorded for the FC mode with the glass SGD.

In light of the above, it is obvious that the operation of an SGD—particularly the Plexiglas SGD—with the new drying mode of CNC is considered a good alternative drying method to an SGD with both the FC and NC drying modes from the thermal and economic perspectives for drying high-moisture content agro-products such as grapes.

Author Contributions: Conceptualization, M.A.T. and M.K.A.E.-W.; methodology, M.A.T., K.M.O. and M.K.A.E.-W.; software, W.E.A.A. validation, M.A.T., K.M.O. and M.K.A.E.-W.; formal analysis, M.A.T., K.M.O. and W.E.A.A.; investigation, M.A.T., K.M.O. and M.K.A.E.-W.; resources, M.A.T. and M.K.A.E.-W.; data curation, M.A.T. and K.M.O.; writing—original draft preparation, M.A.T. and W.E.A.A.; writing—review and editing, M.A.T., K.M.O., M.K.A.E.-W. and W.E.A.A.; supervision M.A.T. and M.K.A.E.-W.; funding acquisition, K.M.O.; All authors have read and agreed to the published version of the manuscript.

Funding: This research received no external funding.

Data Availability Statement: The data will be available through contacting the corresponding author.

Acknowledgments: Authors M.A. Tawfik, Khaled M. Oweda, M.K. Abd El-Wahab and W.E. Abd Allah acknowledge and appreciate the administrative staff of the Faculty of Agriculture, Zagazig University, Egypt, for their support, help and offering all facilities to make this work possible. Additionally, the authors would like to express their deepest thanks and appreciation to Atul A. Sagade, Dept. of Mechanical Engineering, University of Tarapacá, Arica, Chile, for his help and support editing and revising the text of the manuscript.

Conflicts of Interest: The authors declare no conflict of interest.

Nomenclature

A_c	Surface area of the solar air heater/collector (m^2)
A_d	Area of dryer (m^2)
\dot{a}	Experimental constant
\dot{b}	Experimental constant
\dot{c}	Experimental constant
C_{pa}	Specific heat of air (J/kg K)
C_a	Annualized cost (USD)
C_{ac}	Annualized capital cost (USD)
C_{cc}	Capital cost of dryer (USD)
C_d	Drying cost per 1 kg of dried grapes (USD/kg)
C_{ds}	Cost of 1 kg of solar dried grapes (USD/kg)
C_{fg}	Fresh product rate (USD/kg)
$C_{O\&M}$	Annualized operating and maintenance cost (USD)
C_{mar}	Commercial cost of 1 kg of the dried grapes (raisins) in the market (USD)
C_{re}	Annualized running cost (USD)
CRF	Capital recovery factor
D	Number of days for drying in use in one year (days)
DR	Drying rate (kg/kg. h)
D_b	Time taken for drying one batch of grapes sample (h)
d	Inflation rate (%)
h_i	Latent heat of vaporization (kJ/kg)
I_c	Total incident solar radiation intensity on the solar air heater (W/m^2)
I_v	Average incident solar radiation intensity on the dryer (W/m^2)
i	Discount rate (%)
j	Lifespan of the drying system (years)
\dot{k}	Experimental constant
M	Moisture content (g)
M_0	Initial moisture content of product on dry basis (kg water/kg dry matter)
M_b	Mass of dried grapes from one batch (kg)
M_e	Moisture content at equilibrium state on dry basis
M_i	Initial mass of one batch of grapes (kg)
M_t	Moisture content of product at time t on dry basis (kg water/kg dry matter)
MR_{exp}	Experimental moisture ratio, % (wb)
MR_{pre}	Predicted moisture ratio, % (wb)
\dot{m}_a	Mass flow rate of air (kg/s)
m_d	Mass of dry matter (kg)

m_p	Mass of product (kg)
N_p	Payback period (years)
\dot{n}	Experimental constant
P	Annual mass of dried grapes produced by the dryer (kg/year)
R^2	Coefficient of determination
RH_a	Relative humidity of ambient air (%)
RH_g	Relative humidity of air inside the glass dryer(%)
RH_p	Relative humidity of air inside the Plexiglas dryer(%)
S	Salvage value (USD)
S_1	Savings during first year using solar dryer (USD)
S_a	Annualized salvage value (USD/year)
S_{db}	Savings per day during base year using solar dryer (USD)
SFF	Sinking fund factor
T_a	Ambient temperature ($^{\circ}$ C)
T_{ci}	Inlet temperature of solar air heater ($^{\circ}$ C)
T_{co}	Outlet temperature of solar air heater ($^{\circ}$ C)
T_g	Temperature inside the glass dryer ($^{\circ}$ C)
T_p	Temperature inside the Plexiglas dryer ($^{\circ}$ C)
t	Time (s)
χ^2	Chi-squared
Greek symbols	
η_c	Thermal efficiency of solar air heater (%)
η_d	Drying thermal efficiency (%)
Δt	Time interval (h)
Abbreviations	
FC-SGD	Forced convection solar greenhouse dryer
FC	Forced convection
CNC-SGD	Controlled natural convection solar greenhouse dryer
CNC	Controlled natural convection
NC-SGD	Natural convection solar greenhouse dryer
NC	Natural convection
GHG	Greenhouse gases
RH	Relative humidity
RMSE	Root mean square error
SAH	Solar air heater
SGD	Solar greenhouse dryer
SRI	Solar radiation intensity

References

1. Tawfik, M.A.; Sagade, A.A.; Palma-Behnke, R.; Abd Allah, W.E.; Hanan, M. Performance evaluation of solar cooker with tracking type bottom reflector retrofitted with a novel design of thermal storage incorporated absorber plate. *J. Energy Storage* **2022**, *51*, 104432. [CrossRef]
2. United Nations Department of Economic and Social Affairs, Population Division. World Population Prospects 2022: Summary of Results 2022. UN DESA/POP/2022/TR/NO.3. 2022. Available online: <https://reliefweb.int/report/world/world-population-prospects-2022-summary-results> (accessed on 30 July 2022).
3. Tawfik, M.A.; El-Tohamy, M.; Metwally, A.A.; Khallaf, A.M.; Abd Allah, W.E. Experimental and numerical investigation of thermal performance of a new design solar parabolic dish desalination system. *Appl. Therm. Eng.* **2022**, *214*, 118827. [CrossRef]
4. Kant, K.; Shukla, A.; Sharma, A.; Kumar, A.; Jain, A. Thermal energy storage based solar drying systems: A review. *Innov. Food Sci. Emerg. Technol.* **2016**, *34*, 86–99. [CrossRef]
5. Moses, J.A.; Norton, T.; Alagusundaram, K.; Tiwari, B.K. Novel drying techniques for the food industry. *Food Eng. Rev.* **2014**, *6*, 43–55. [CrossRef]
6. Mugi, V.R.; Chandramohan, V.P. Energy, exergy and economic analysis of an indirect type solar dryer using green chilli: A comparative assessment of forced and natural convection. *Therm. Sci. Eng. Prog.* **2020**, *24*, 100950. [CrossRef]
7. Sethi, V.P.; Dhiman, M. Design, space optimization and modelling of solar-cum-biomass hybrid greenhouse crop dryer using flue gas heat transfer pipe network. *Sol. Energy* **2020**, *206*, 120–135. [CrossRef]
8. Patil, R.; Gawande, R.A. Review on solar tunnel greenhouse drying system. *Renew. Sustain. Energy Rev.* **2016**, *56*, 196–214. [CrossRef]

9. Rabha, D.K.; Muthukumar, P. Performance studies on a forced convection solar dryer integrated with a paraffin wax-based latent heat storage system. *Sol. Energy* **2017**, *149*, 214–226. [[CrossRef](#)]
10. Saini, V.; Tiwari, S.; Tiwari, G.N. Environ economic analysis of various types of photovoltaic technologies integrated with greenhouse solar drying system. *J. Clean. Prod.* **2017**, *156*, 30–40. [[CrossRef](#)]
11. Mohana, Y.; Mohanapriya, R.; Anukiruthika, T.; Yoha, K.S.; Moses, J.A.; Anandharamakrish, C. Solar dryers for food applications: Concepts, designs, and recent advances. *Sol. Energy* **2020**, *208*, 321–344. [[CrossRef](#)]
12. Debnath, S.; Das, B.; Randive, P.R.; Pandey, K.M. Performance analysis of solar air collector in the climatic condition of North Eastern India. *Energy* **2018**, *165*, 281–298. [[CrossRef](#)]
13. Kumar, P.; Singh, D. Advanced technologies and performance investigations of solar dryers: A review. *Renew. Energy Focus* **2020**, *35*, 148–158. [[CrossRef](#)]
14. Nukulwar, M.R.; Tungikar, V.B. A review on performance evaluation of solar dryer and its material for drying agricultural products. *Mater. Today Proc.* **2021**, *46*, 345–349. [[CrossRef](#)]
15. Tiwari, S.; Tiwari, G.; Al-Helal, I. Development and recent trends in greenhouse dryer: A review. *Renew. Sustain. Energy Rev.* **2016**, *65*, 1048–1064. [[CrossRef](#)]
16. Vivekanandan, M.; Periasamy, K.; Babu, C.D.; Selvakumar, G.; Arivazhagan, R. Experimental and CFD investigation of six shapes of solar greenhouse dryer in no load conditions to identify the ideal shape of dryer. *Mater. Today Proc.* **2021**, *37*, 1409–1416. [[CrossRef](#)]
17. Lamrani, B.; Draoui, A.; Kuznik, F. Thermal performance and environmental assessment of a hybrid solar-electrical wood dryer integrated with Photovoltaic/Thermal air collector and heat recovery system. *Sol. Energy* **2021**, *221*, 60–74. [[CrossRef](#)]
18. Kumar, R.; Rosen, M.A. A critical review of photovoltaic-thermal solar collectors for air heating. *Appl. Energy* **2011**, *88*, 3603–3614. [[CrossRef](#)]
19. César, L.-V.E.; Lilia, C.-M.A.; Octavio, G.-V.; Orlando, S.S.; Alfredo, D.N. Energy and exergy analyses of a mixed-mode solar dryer of pear slices (*Pyrus communis* L.). *Energy* **2021**, *220*, 119740. [[CrossRef](#)]
20. Chauhan, Y.B.; Rathod, P.P. A comprehensive review of the solar dryer. *Int. J. Ambient Energy* **2020**, *41*, 348–367. [[CrossRef](#)]
21. Tiwari, S.; Tiwari, G.N. Energy and exergy analysis of a mixed-mode greenhouse-type solar dryer, integrated with partially covered N-PVT air collector. *Energy* **2017**, *128*, 183–195. [[CrossRef](#)]
22. Bal, L.M.; Satya, S.; Naik, S.N. Solar dryer with thermal energy storage systems for drying agricultural food products: A review. *Renew. Sustain. Energy Rev.* **2010**, *14*, 2298–2314. [[CrossRef](#)]
23. Murthy, M.V.R. A review of new technologies, models and experimental investigations of solar driers. *Renew. Sustain. Energy Rev.* **2009**, *13*, 835–844. [[CrossRef](#)]
24. Srinivasan, G.; Muthukumar, P. A review on solar greenhouse dryer: Design, thermal modelling, energy, economic and environmental aspects. *Sol. Energy* **2021**, *229*, 3–21. [[CrossRef](#)]
25. Gorjian, S.; Hosseingholilou, B.; Jathar, L.D.; Samadi, H.; Samanta, S.; Sagade, A.A.; Kant, K.; Sathyamurthy, R. Recent advancements in technical design and thermal performance enhancement of solar greenhouse dryers. *Sustainability* **2021**, *13*, 7025. [[CrossRef](#)]
26. Chauhan, P.S.; Kumar, A. Performance analysis of greenhouse dryer by using insulated north-wall under natural convection mode. *Energy Rep.* **2016**, *2*, 107–116. [[CrossRef](#)]
27. Kumar, M.; Sahdev, R.K.; Tiwari, S.; Manchanda, H.; Chhabra, D.; Panchal, H.H.; Sadasivuni, K.K. Thermal performance and kinetic analysis of vermicelli drying inside a greenhouse for sustainable development. *Sustain. Energy Technol. Assess.* **2021**, *44*, 101082. [[CrossRef](#)]
28. Chauhan, P.S.; Kumar, A.; Gupta, B. A review on thermal models for greenhouse dryers. *Renew. Sustain. Energy Rev.* **2017**, *75*, 548–558. [[CrossRef](#)]
29. Prakashm, O.; Kumar, A. Historical review and recent trends in solar drying systems. *Int. J. Green Energy* **2013**, *10*, 690–738. [[CrossRef](#)]
30. Singh, S.; Gill, R.S.; Hans, V.S.; Mittal, T.C. Experimental performance and economic viability of evacuated tube solar collector assisted greenhouse dryer for sustainable development. *Energy* **2022**, *241*, 122794. [[CrossRef](#)]
31. ELkhadraoui, A.; Kooli, S.; Hamdi, I.; Farhat, A. Experimental investigation and economic evaluation of a new mixed-mode solar greenhouse dryer for drying of red pepper and grape. *Renew. Energy* **2015**, *77*, 1–8. [[CrossRef](#)]
32. Janjai, S.; Intawee, P.; Kaewkiewa, J.; Sritus, C.; Khamvongsa, V. A large-scale solar greenhouse dryer using polycarbonate cover: Modeling and testing in a tropical environment of Lao People’s Democratic Republic. *Renew. Energy* **2011**, *36*, 1053–1062. [[CrossRef](#)]
33. Chauhan, P.S.; Kumar, A.; Nuntadusit, C. Thermo-environmental and drying kinetics of bitter melon flakes drying under north wall insulated greenhouse dryer. *Sol. Energy* **2018**, *162*, 205–216. [[CrossRef](#)]
34. Prakash, O.; Kumar, A. Annual performance of a modified greenhouse dryer under passive mode in no-load conditions. *Int. J. Green Energy* **2015**, *12*, 1091–1099. [[CrossRef](#)]
35. Prakash, O.; Kumar, A. Solar greenhouse drying: A review. *Renew. Sustain. Energy Rev.* **2014**, *29*, 905–910. [[CrossRef](#)]
36. Karthikeyan, M.G.; Lavanya, M.V.; Dharani, M.N.; Nagulan, M.T. Grapes (*Vitis vitaceae*)-potent medicinal fruit serves as a source of antioxidants and antibacterial agent. *Int. J. Curr. Sci. Res. Rev.* **2020**, *3*, 70–81. [[CrossRef](#)]

37. Sehery, A.A.; Gallali, Y.M.; Wafa, M.J. Preservation of Fruits and Vegetables Using Solar Dryers. A Comparative Study for Solar and Natural Drying of Grapes, Figs, Tomatoes and Onions. IV. Temperatu. In *World Renewable Energy Congress VI*; Pergamon: Brighton, UK, 2000; pp. 2167–2169.
38. Gallali, Y.M.; Abujnah, Y.S.; Bannani, F.K. Preservation of fruits and vegetables using solar drier: A comparative study of natural and solar drying, III, chemical analysis and sensory evaluation data of the dried samples (grapes, figs, tomatoes and onions). *Renew. Energy* **2000**, *19*, 203–212. [[CrossRef](#)]
39. Yaldiz, O.; Ertekin, C.; Uzun, H.I. Mathematical modeling of thin layer solar drying of sultana grapes. *Energy* **2001**, *26*, 457–465. [[CrossRef](#)]
40. Al-Juamili, K.E.; Khalifa, A.J.N.; Yassen, T.A. Testing of the performance of a fruit and vegetable solar drying system in Iraq. *Desalination* **2007**, *209*, 163–170. [[CrossRef](#)]
41. Essalhi, H.; Benchrif, M.; Tadili, R.; Bargach, M.N. Experimental and theoretical analysis of drying grapes under an indirect solar dryer and in open sun. *Innov. Food Sci. Emerg. Technol.* **2018**, *49*, 58–64. [[CrossRef](#)]
42. Sharma, V.K.; Colangelo, A.; Spagna, G. Experimental performance of an indirect type solar fruit and vegetable dryer. *Energy Convers. Manag.* **1993**, *34*, 293–308. [[CrossRef](#)]
43. Tiris, C.; Ozbalta, N.; Tiris, M.; Dincer, I. Performance of a solar dryer. *Energy* **1994**, *19*, 993–997. [[CrossRef](#)]
44. Tiris, C.; Tiris, M.; Dincer, I. Investigation of the thermal efficiencies of a solar dryer. *Energy Convers. Manag.* **1995**, *36*, 205–212. [[CrossRef](#)]
45. Zomorodian, A.; Dadashzadeh, M. Indirect and mixed mode solar drying mathematical models for sultana grape. *J. Agric. Sci. Technol.* **2009**, *11*, 391–400.
46. Pardhi, C.B.; Bhagoria, J.L. Development and performance evaluation of mixed-mode solar dryer with forced convection. *Int. J. Energy Environ. Eng.* **2013**, *4*, 23. [[CrossRef](#)]
47. El-Sebaei, A.A.; Aboul-Enein, S.; Ramadan, M.R.I.; El-Gohary, H.G. Experimental investigation of an indirect type natural convection solar dryer. *Energy Convers. Manag.* **2002**, *43*, 2251–2266. [[CrossRef](#)]
48. Papade, C.V.; Boda, M.A. Design and development of indirect type solar dryer with energy storing material. *Int. J. Innov. Res. Adv. Eng.* **2014**, *1*, 109–114.
49. Fuller, R.J.; Charters, W.W.S. Performance of a solar tunnel dryer with microcomputer control. *Sol. Energy* **1997**, *59*, 151–154. [[CrossRef](#)]
50. Barnwal, P.; Tiwari, G.N. Grape drying by using hybrid photovoltaic-thermal (PV/T) greenhouse dryer: An experimental study. *Sol. Energy* **2008**, *82*, 1131–1144. [[CrossRef](#)]
51. Rathore, N.S.; Panwar, N.L. Experimental studies on hemi cylindrical walk-in type solar tunnel dryer for grape drying. *Appl. Energy* **2010**, *87*, 2764–2767. [[CrossRef](#)]
52. Hamdi, I.; Kooli, S.; Elkhadraoui, A.; Azaizia, Z.; Abdelhamid, F.; Guizani, A. Experimental study and numerical modeling for drying grapes under solar greenhouse. *Renew. Energy* **2018**, *127*, 936–946. [[CrossRef](#)]
53. Tiwari, S.; Tiwari, G.N.; Al-Helal, I.M. Performance analysis of photovoltaic-thermal (PVT) mixed mode greenhouse solar dryer. *Sol. Energy* **2016**, *133*, 421–428. [[CrossRef](#)]
54. Gopinath, G.R.; Muthuvel, S.; Muthukannan, M.; Sudhakarapandian, R.; Kumar, B.P.; Kumar, C.S.; Thanikanti, S.B. Design, development, and performance testing of thermal energy storage based solar dryer system for seeded grapes. *Sustain. Energy Technol. Assess.* **2022**, *51*, 101923. [[CrossRef](#)]
55. Nagarajan, S.; Prem Kumar, M. Analysis of Thermal Performance in Solar Dryer. *IOSR J. Mech. Civ. Eng.* **2022**, *11*, 71–74.
56. Di Matteo, M.; Cinquanta, L.; Galiero, G.; Crescitelli, S. Effect of a novel physical pretreatment process on the drying kinetics of seedless grapes. *J. Food Eng.* **2000**, *46*, 83–89. [[CrossRef](#)]
57. Pangavhane, D.R.; Sawhney, R.L.; Sarsavadia, P.N. Effect of various dipping pretreatment on drying kinetics of Thomson seedless grapes. *J. Food Eng.* **1999**, *39*, 211–216. [[CrossRef](#)]
58. Richard, J.M.; Bernadette, K.N.; Trude, W.; Lucy, M.C.; Bernard, E.C. Effect of solar drying methods on total phenolic contents and antioxidant activity of commonly consumed fruits and vegetable (mango, banana, pineapple and tomato) in Tanzania. *Afr. J. Food Sci.* **2015**, *9*, 291–300. [[CrossRef](#)]
59. Saxena, A.; Cuce, E.; Singh, D.B.; Sethi, M.; Cuce, P.M.; Sagade, A.A.; Kumar, A. Experimental studies of latent heat storage based solar air heater for space heating: A comparative analysis. *J. Build. Eng.* **2023**, *69*, 106282. [[CrossRef](#)]
60. Aghbashlo, M.; Kianmehr, M.H.; Arabhosseini, A. Modelling of thin layer drying of potato slices in length of continuous band dryer. *Energy Convers. Manag.* **2009**, *50*, 1348–1355. [[CrossRef](#)]
61. Midilli, A.; Kucuk, H. Mathematical modeling of thin layer drying of pistachio by using solar energy. *Energy Convers. Manag.* **2003**, *44*, 1111–1122. [[CrossRef](#)]
62. Lingayat, A.; Chandramohan, V.P.; Raju, V.R.K.; Suresh, S. Drying kinetics of tomato (*Solanum lycopersicum*) and Brinjal (*Solanum melongena*) using an indirect type solar dryer and performance parameters of dryer. *Heat Mass Transf.* **2021**, *57*, 853–872. [[CrossRef](#)]
63. Kesavan, S.; Arjunan, T.V.; Vijayan, S. Thermodynamic analysis of a triple-pass solar dryer for drying potato slices. *J. Therm. Anal. Calorim.* **2019**, *136*, 159–171. [[CrossRef](#)]
64. Cesar, L.V.E.; Ana Lilia, C.M.; Octavio, G.V.; Isaac, P.F.; Rogelio, B.O. Thermal performance of a passive, mixed-type solar dryer for tomato slices (*Solanum lycopersicum*). *Renew. Energy* **2020**, *147*, 845–855. [[CrossRef](#)]
65. Henderson, S.M.; Pabis, S. Grain drying theory I. temperature effect on drying coefficient. *J. Agric. Eng. Res.* **1961**, *6*, 169–174.

66. Ozdemir, M.; Devres, Y.O. The thin layer drying Characteristics of hazelnuts during roasting. *J. Food. Eng.* **1999**, *42*, 225–233. [[CrossRef](#)]
67. Sharma, G.P.; Prasad, S. Effective Moisture Diffusivity of Garlic Cloves Undergoing Microwave Convective Drying. *J. Food Eng.* **2004**, *65*, 605–617. [[CrossRef](#)]
68. Kumar, M.; Sahdev, R.K.; Tawfik, M.A.; Elboughdiri, N. Natural convective greenhouse vermicelli drying: Thermo-viron-econo-kinetic analyses. *Sustain. Energy Technol. Assess.* **2023**, *55*, 103002. [[CrossRef](#)]
69. Badaoui, O.; Hanini, S.; Djebli, A.; Brahim, H.; Benhamou, A. Experimental and modeling study of tomato pomace waste drying in a new solar greenhouse: Evaluation of new drying models. *Renew. Energy* **2019**, *133*, 144–155. [[CrossRef](#)]
70. Deng, S.; Wen, Z.; Su, F.; Wang, Z.; Lou, G.; Liu, X.; Dou, R. Converter sludge drying in rotating drum using hot steel balls. *Appl. Therm. Eng.* **2021**, *197*, 117368. [[CrossRef](#)]
71. Dharmadurai, P.L.; Vasanthaseelan, S.; Bharathwaaj, R.; Dharmaraj, V.; Gnanasekaran, K.; Balaji, D.; Sathyamurthy, R. A comparative study on solar dryer using external reflector for drying grapes. *Mater. Today Proc.* **2022**, *50*, 552–559. [[CrossRef](#)]
72. Singh, P.P.; Singh, S.; Dhaliwal, S.S. Multi-shelf domestic solar dryer. *Energy Convers. Manag.* **2006**, *47*, 1799–1815. [[CrossRef](#)]
73. Sodha, M.S.; Chandra, R.; Pathak, K.; Singh, N.P.; Bansal, N.K. Techno-economic analysis of typical dryers. *Energy Convers. Manag.* **1991**, *31*, 503–5013. [[CrossRef](#)]
74. Akpınar, E.K. Drying of mint leaves in a solar dryer and under open sun: Modelling, performance analyses. *Energy Convers. Manag.* **2010**, *51*, 2407–2418. [[CrossRef](#)]

Disclaimer/Publisher’s Note: The statements, opinions and data contained in all publications are solely those of the individual author(s) and contributor(s) and not of MDPI and/or the editor(s). MDPI and/or the editor(s) disclaim responsibility for any injury to people or property resulting from any ideas, methods, instructions or products referred to in the content.